Article

Not peer-reviewed version

Between Surprises and Novelties: Benzyl Triphenyl Phosphonium Bromide Is Bactericidal Against MRSA and Inhibits Biofilm Formation with Minimal Cytotoxicity

Silvana Alfei *, Gabriella Piatti, Guendalina Zuccari, Caterina Reggio, Anna Maria Schito *

Posted Date: 6 March 2026

doi: 10.20944/preprints202603.0534.v1

Keywords: multidrug resistant bacteria; triphenyl phosphonium (TPP) group; minimum inhibitory concentration (MIC); bacteriostatic and bactericidal effects; time-killing experiments

 doi:10.20944/preprints202603.0534.v1

Article

Between Surprises and Novelties: Benzyl Triphenyl Phosphonium Bromide Is Bactericidal Against MRSA and Inhibits Biofilm Formation with Minimal Cytotoxicity

Silvana Alfei [1,*], Gabriella Piatti [2], Guendalina Zuccari [1,3,*], Caterina Reggio [3] and Anna Maria Schito [2,*]

[1] Department of Pharmacy (DIFAR), University of Genoa, Viale Cembrano, 4, 16148 Genoa, Italy

[2] Department of Surgical Sciences and Integrated Diagnostics (DISC), University of Genoa, Viale Benedetto XV, 6, 16132 Genova, Italy

[3] Laboratory of Experimental Therapies in Oncology, IRCCS Istituto Giannina Gaslini, Via G. Gaslini 5, 16147 Genoa, Italy

* Correspondence: alfei@difar.unige.it (S.A.); amschito@unige.it (A.M.S.); Tel.: +39 010 355 2296 (S.A.)

Abstract

Background. Quaternary phosphonium salts (QPSs) are extensively researched since represent new promising weapons to counteract critical superbugs, regardless their robust pattern of resistance. **Methods.** Here, dynamic light scattering analysis was carried out on QPSs **1**, **3** and **4** recently reported and already found active against cancer cells, and phosphine **2** unveiling particles of 700-800 nm for **2**, **3** and **4** and positive Zeta-potential (ζ-p) for all (+4.2-+38.1 mV). **1**, **3** and **4** plus **2**, were microbiologically evaluated, assessing minimum inhibitory concentration values (MICs) (**1**-**4**), time-killing curves (**1**), and anti-biofilm capacity (**1**). **Results.** MICs on a total of 23 Gram-positive and Gram-negative clinically isolated superbugs, evidenced that, poorly soluble **2**, **3** and **4** exhibited not reproducible MICs, while **1** provided interesting MICs, which made it worthy of further investigations. In fact, **1** was active against clinically relevant multidrug-resistant (MDR) Gram-positive species and not active against MDR Gram-negative species including *Pseudomonas aeruginosa*. Specifically, MICs = 16-32 μg/mL and 16-64 μg/mL were determined against methicillin-resistant *Staphylococcus aureus* (MRSA) and *S. epidermidis* (MRSE) respectively. MICs = 32-64 μg/mL were observed against teicoplanin- and vancomycin-resistant (VRE) *Enterococcus faecalis* and *E. faecium* and no activity against *P. aeruginosa* (> 128 μg/mL). Notably, time-kill experiments established that **1** was bactericidal against MRSA, while strongly inhibited (up to 100%) the formation of biofilm produced by the strongest biofilm-producers *S. epidermidis* and *S. aureus* isolates of our collection, at MICs and 2.5 × MIC concentrations, depending on isolates considered. Interestingly, if used against *Staphylococci*, and mainly MRSA, **1** was softly haemolytic. It was no cytotoxic against not tumorigenic human keratinocytes (HaCaT) and murine embryonic fibroblasts (3T3) in all cases. Structure-activity relationships have been studied, leading to outcomes which could be of great help for designing optimized new QPSs. **Conclusions.** Findings of this study overturn previous antimicrobial reports on compound **1**, suggesting it as a new excellent weapon to counteract bacterial resistance and biofilm production by MRSA and MRSE superbugs, as well as thinkable for future in vivo experiments and clinical development.

Keywords: multidrug resistant bacteria; triphenyl phosphonium (TPP) group; minimum inhibitory concentration (MIC); bacteriostatic and bactericidal effects; time-killing experiments

1. Introduction

 doi:10.20944/preprints202603.0534.v1

The overprescription and misuse of antibiotics in both humans and animals, their use without proper medical indication, poor drug quality, and patients' failure to complete the full course of treatment strongly promote genetic mutations in microorganisms, leading to the development of resistance to multiple antibiotics [1]. In this context, multidrug resistant (MDR) superbugs are pathogens that have developed resistance to multiple classes of antibiotics, sometimes to all available treatments. This virulence worryingly is leading to difficult-to-treat infections, associated with prolonged hospitalization, increased morbidity and mortality, and significant economic burden[1]. Poor hygiene and scarce sanitation of certain geographic areas can further worsen an already critical scenario [2].

The World Health Organization (WHO) predicted already years ago (2021), that without new and better treatments, the number of deaths caused by superbugs could rise to 10 million by 2050, highlighting a health concern of paramount importance [3].

MDR strains primarily emerge in hospital settings, where severely immunocompromised and long-term hospitalized patients are particularly susceptible to colonization by opportunistic pathogens. These infections often progress to severe clinical conditions requiring aggressive and prolonged therapeutic regimens [4]. These superbugs are responsible for a high percentage of hospital-acquired infections and can turn otherwise treatable conditions—such as pneumonia, bloodstream infections, and urinary tract infections—into life-threatening diseases. They are particularly dangerous for vulnerable patients, including individuals with diabetes, severe burn injuries, organ transplants, and other compromised health conditions [5]. According to WHO priority list of antibiotic-resistant bacteria, particular concern is associated with methicillin-resistant *Staphylococcus aureus* (MRSA) and vancomycin-resistant *Enterococcus faecium* (VRE), both classified among high-priority pathogens [5]. In addition, methicillin-resistant *Staphylococcus epidermidis* (MRSE) has emerged as a significant nosocomial pathogen due to its increasing multidrug resistance and strong biofilm-forming ability. The global spread of MRSA, MRSE, and VRE highlights their clinical relevance and underscores the urgent need for improved surveillance, infection control strategies, and the development of novel antimicrobial therapies.

MRSA represents one of the most clinically relevant MDR pathogens worldwide. Originally confined to healthcare settings (HA-MRSA), it has now spread extensively into the community (CA-MRSA), causing a broad spectrum of diseases ranging from skin and soft tissue infections to invasive conditions such as bacteraemia, osteoarticular infections, and endocarditis [4]. Its resistance is primarily mediated by the acquisition of the *mecA* gene, encoding the altered penicillin-binding protein PBP2a, which confers resistance to all β-lactam antibiotics [5,6]. MRSA infections are associated with increased morbidity, mortality, prolonged hospitalization, and higher healthcare costs. The pathogen's ability to form biofilms and to acquire additional resistance determinants further complicates treatment, limiting therapeutic options to agents such as vancomycin, linezolid, daptomycin, and newer anti-MRSA compounds[7,8]. The global dissemination of MRSA continues to represent a major public health challenge and novel therapeutic approaches targeting biofilm and resistance mechanisms are actively being investigated to improve clinical outcomes.

S. epidermidis is the most prevalent coagulase-negative *Staphylococcus* species colonizing human skin and mucosal surfaces. In its natural ecological niche, it is generally harmless and acts as a commensal organism. However, it can become an opportunistic pathogen when introduced into the body through medical devices such as intravascular catheters, prosthetic heart valves, cardiac devices, orthopaedic implants, and cerebrospinal fluid shunts [9,10]. In these settings, *S. epidermidis* can cause both localized and systemic infections, often associated with significant clinical complications. Of particular concern is the increasing prevalence of MRSE *S. epidermidis*, which, like MRSA [11,12]. This resistance markedly limits therapeutic options and complicates clinical management. A major virulence factor of this species is its ability to form biofilms on abiotic surfaces, which enhances bacterial persistence by protecting cells from host immune responses and antimicrobial therapy, thereby rendering infections particularly difficult to eradicate [13].

 doi:10.20944/preprints202603.0534.v1

Enterococci, particularly *E. faecalis* and *E. faecium*, are among the most significant opportunistic pathogens in clinical settings. Although they are normal inhabitants of the human gastrointestinal tract, they have emerged as leading causes of healthcare-associated infections. Enterococci are commonly implicated in urinary tract infections, bacteraemia, endocarditis, intra-abdominal infections, and device-associated infections [14,15]. Their clinical relevance is largely attributable to intrinsic resistance to several antibiotic classes, including cephalosporins and low levels of aminoglycosides, and their remarkable ability to acquire additional resistance determinants. Of particular concern is the global spread of vancomycin-resistant enterococci (VRE), which significantly limits therapeutic options and is associated with increased morbidity, mortality, and healthcare costs[16]. Furthermore, enterococci can form biofilms on medical devices, contributing to persistent and difficult-to-treat infections[17]. Their adaptability and resistance profile make them a major public health concern worldwide. The currently available therapeutic armamentarium against these multidrug-resistant pathogens remains limited. Today's clinical management of infections caused by MRSA, MRSE, and VRE is increasingly challenging, as multidrug resistance reduces the effectiveness of cornerstone agents such as vancomycin, linezolid, and daptomycin, promotes persistent biofilm-associated and device-related infections, and often necessitates combination regimens or the use of newer agents supported by variable clinical evidence. These limitations highlight the urgent need for optimized antimicrobial stewardship and the development of innovative therapeutic strategies targeting resistance and biofilm mechanisms.

To meet these needs, we considered QPSs **1**, **3** and **4**, already found active against cancer cells, and low cytotoxic versus human keratinocytes (HaCaT) and murine fibroblasts (3T3) eukaryotic cells[18]. For reasons better detailed in the subsequent Section 1.1, they appear as good candidates to have also antibacterial properties. Not cationic phosphine compound **2**, available since synthesized as precursor for achieving compounds **3** and **4** was also investigated. While with some questionable results, to be verified, the antibacterial effects of compound **1** were already reported [19], compounds **2**, **3** and **4** were never microbiologically tested. **1**, **3**, **4** and **2** were finally tested against a selection of 23 Gram-positive and Gram-negative superbugs, except for *S. aureus* ATCC, a very complex pattern of cross-resistance. No reliable MICs for **2**, **3** and **4** were observed, due to their poor solubility, which forced us to not further consider, for the moment, such compounds. Conversely, very promising results were obtained for compound **1**, which were in substantial contrast with those by other authors, who previously evaluated it [19]. Despite not active for our standards, against all Gram-negative MDR isolates tested in this study (7 strains), 1 demonstrated from moderate to good activity against all Gram-positive strains used here (15 MDR superbugs and 1 ATCC strain), regardless their resistance profile. As first novelty regarding **1**, time killing curves were determined at 24 hours from inoculum using different MRSA isolates to establish its bacteriostatic or bactericidal behaviour. As second one, experiments assessing its capacity to inhibit biofilm formation were carried out using four *plus* four clinical MRSA and MRSE isolates among the strongest biofilm-producers of our collection (OD_{570} up to >>> 3).

Structure-activity relationships considerations have been reported, which in part confirmed and in part provided new information about groups needed, not advisable or not suggestable contemporarily in the phosphonium salt's structures to have substantial antibacterial effects.

1.1. Why Phosphonium Salts 1, 3 and 4, as well as Phosphine 2 Were Chosen for Antimicrobial Experiments in this Study?

Cationic compounds often exhibit dual antibacterial and anticancer activity, due to their ability to selectively interact with negatively charged cell membranes. Several studies show that the positive charge promotes electrostatic attraction to the surfaces of both bacteria and tumour cells, both characterized by a high density of anionic groups. This interaction leads to permeabilization, destabilization of the lipid bilayer, and cell death. Recent reviews emphasize that many cationic antimicrobial peptides, originally designed for antibacterial activity, can be repurposed as anticancer agents (or *vice versa*) precisely because they share the same membrane-disruptive[20,21]. It has also

 doi:10.20944/preprints202603.0534.v1

been observed that surface charge neutralization and pore formation induced by cationic peptides or nanoparticles represent a common mechanism that explains their efficacy against resistant bacteria and highly aggressive tumour cells[22,23]. This mechanistic convergence makes cationic compounds a particularly promising platform for dual-action therapeutic strategies. In this regard, QPSs **1**, **3** and **4** were recently found to have considerable anticancer effects [18] and therefore could be excellent candidates to have also antibacterial effects. A confirmation of a rational choice derived by accurate research among literature reports. Specifically, although commercial tetraphenyl phosphonium chloride [TPP][Cl] (98%), ethyl-triphenyl phosphonium iodide [ETPP][I] (95%) and tri-hexyl tetradecyl phosphonium chloride [TTP][Cl] (95%) demonstrated absent to scarce bactericidal effects against *E. coli* (MBCs = 1750, 1500 and 100 μg/mL) [24], several polymeric and not polymeric quaternized phosphonium salts (PQPSs and QPSs) have showed to possess from narrow to broad-spectrum remarkable antibacterial/bactericidal effects, acting a-specifically, as membrane disruptors, thus circumventing bacterial resistance [25–33]. Both poorly packed and highly hindered tetra alkyl phosphonium salts (TAPILs), as well as tri phenyl phosphonium salts, containing $[PR_4]^+$ or $[PPh_3R]^+$ (R = alkyl chains) cations and an inorganic or organic anions respectively, have demonstrated antibacterial activity depending on the anion, the length of alkyl chains and their hindrance. Depending on their structure, such compounds demonstrated from moderate to potent antibacterial effects against *S. aureus*, *E. coli*, *S. epidermidis*, *E. faecium*, MRSA and *Acinetobacter Baumannii*, sometimes comparable to that of a standard commercial biocide, such as benzalkonium chloride and commercial surfactant Triton-X-100 [31,33–37]. Specifically, *bis*-phosphonium ionic liquids demonstrated antimicrobial effects versus important eye pathogens, such as MDR *P. aeruginosa*, and ocular fungal isolates, despite being affected by high corneal cytotoxicity [38]. Also, C3-C7 trialkyl phosphonium derivatives, with a complex fourth substituent on phosphorous atoms, demonstrated notable antibacterial activity against *Bacillus subtilis* with pronounced uncoupling activity in isolated rat liver mitochondria [39]. Additionally, reviews on the antimicrobial properties of other classes of ionic liquids, active also against biofilm formation were found, which gave us interesting indications [40,41]. Additionally, although Ermolaev et al. preferred the tri-*tert*-butyl group to the triphenyl phosphonium (TPP) group [31], TPP, benzyl and alkyl benzyl diphenyl phosphonium (DPP) molecules have been found to possess antibacterial activity especially against Gram-positive standard strains from American Type Culture Collection (ATCC) and clinical isolates [19,42,43]. The remarkable antibacterial effect of a 11-hydroxyalkyl-mono-triphenyl phosphonium salt (TPPOH) against MDR Gram-positive species and the even more potent bacteriostatic and anticancer effects of a bola-amphiphilic 1-12-*bis*-triphenyl phosphonium undecane bromide (BPPB) against both MDR Gram-positive and negative species [26,27], associated with soft cytotoxicity against eukaryotic cells and RBCs were recently reported [27,44–47]. Finally, the pivotal role of using the triphenyl phosphonium (TPP) group-containing hexanoate, to chemically modify certain inactive triterpenoids, thus conferring them antibacterial effects of against MRSA, MRSE and vancomycin resistant (VRE) enterococci also resistant to teicoplanin, has been very recently demonstrated [28]. On these findings, our choice to try **1**, usually used in organic synthesis, as a phase transfer catalyst, a Wittig reagent, and a Michael acceptor, but also applied in the production of pharmaceuticals, agrochemicals, and polymers, in antibacterial experiments revealed to be rational. Similarly, also the choice of testing other two anticancer compounds (**3**, **4**), not having the TPP group, but alkyl chains encompassing both ten carbon atoms, but different hydrophilic-hydrophobic balances, respecting the length usually reported to confer antibacterial activity, and phenyl benzyl structures, was confirmed to be rational. Collectively, no chosen compound contained simultaneously the TPP-group and the alkyl chain, as for the most active compounds previously reported [26,27,33] or contained the hindering well-functioning tetra alkyl groups reported by Ermolaev et al. [31]. This strategy would have revealed if the simultaneous presence of the TPP group and of the alkyl chain, present in **3** and **4** but not in **1**, which conversely contained TPP but not the chain, is strictly necessary for having consistent antibacterial effects or TPP alone could be sufficient. Compound **2**, which was primarily synthesized because needed to achieve **3** and **4**, despite not quaternized and not cationic, was also

 doi:10.20944/preprints202603.0534.v1

tested, since it demonstrated to be nanosized and with the highest positive ζ-p of 15.7 mV, which could have anyway promoted interactions with bacterial surface, thus impairing bacterial membranes functions, and causing pathogens inhibition/death.

2. Results and Discussion

2.1. Synthesis of Quaternary Benzyl Phosphonium Bromides 1, 3 and 4

Chemical structures of phosphonium bromides **1**, **3** and **4**, as well as that of compound **2**, synthesized since precursor needed to achieve **3** and **4** have been shown in Chart 1.

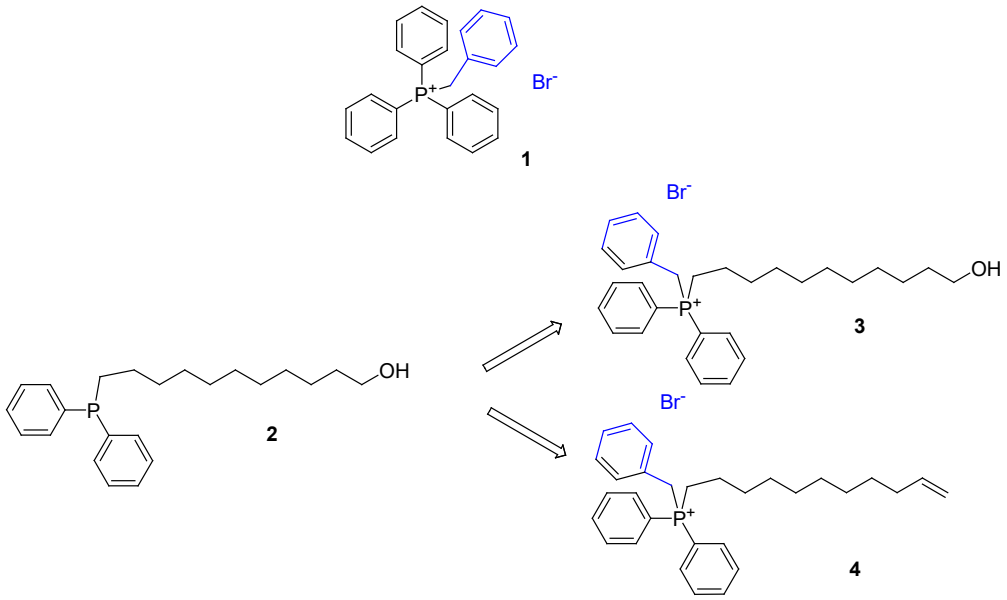

Chart 1. Chemical structures of compounds **1**-**4**. Not quaternized compound **2** was prepared since precursor needed for achieving compounds **3** and **4**.

Quaternized phosphonium salts **1**, **3**, **4** and tertiary phosphine derivative **2** were synthetized according to Scheme 1A, 1B, and 1C, performing procedures recently described[18].

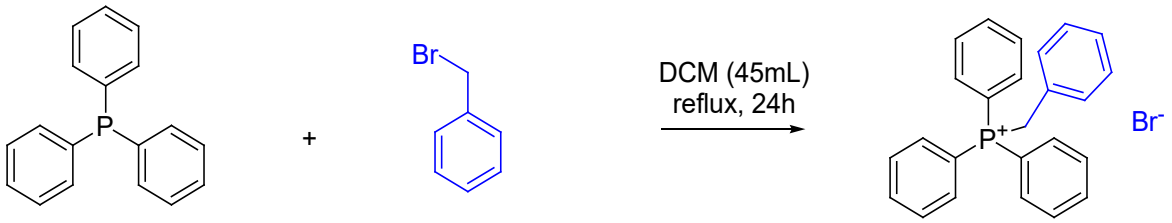

$C_{18}H_{15}P$
269.09
1.35 g, 5.02 mmol

C_7H_7Br
171.03/d = 1.438 g/cm^3
0.85 g, 4.97 mmol, 0.6 mL

$C_{25}H_{22}PBr$
433.32
M.p.: 241°C (lit)

(A)

 doi:10.20944/preprints202603.0534.v1

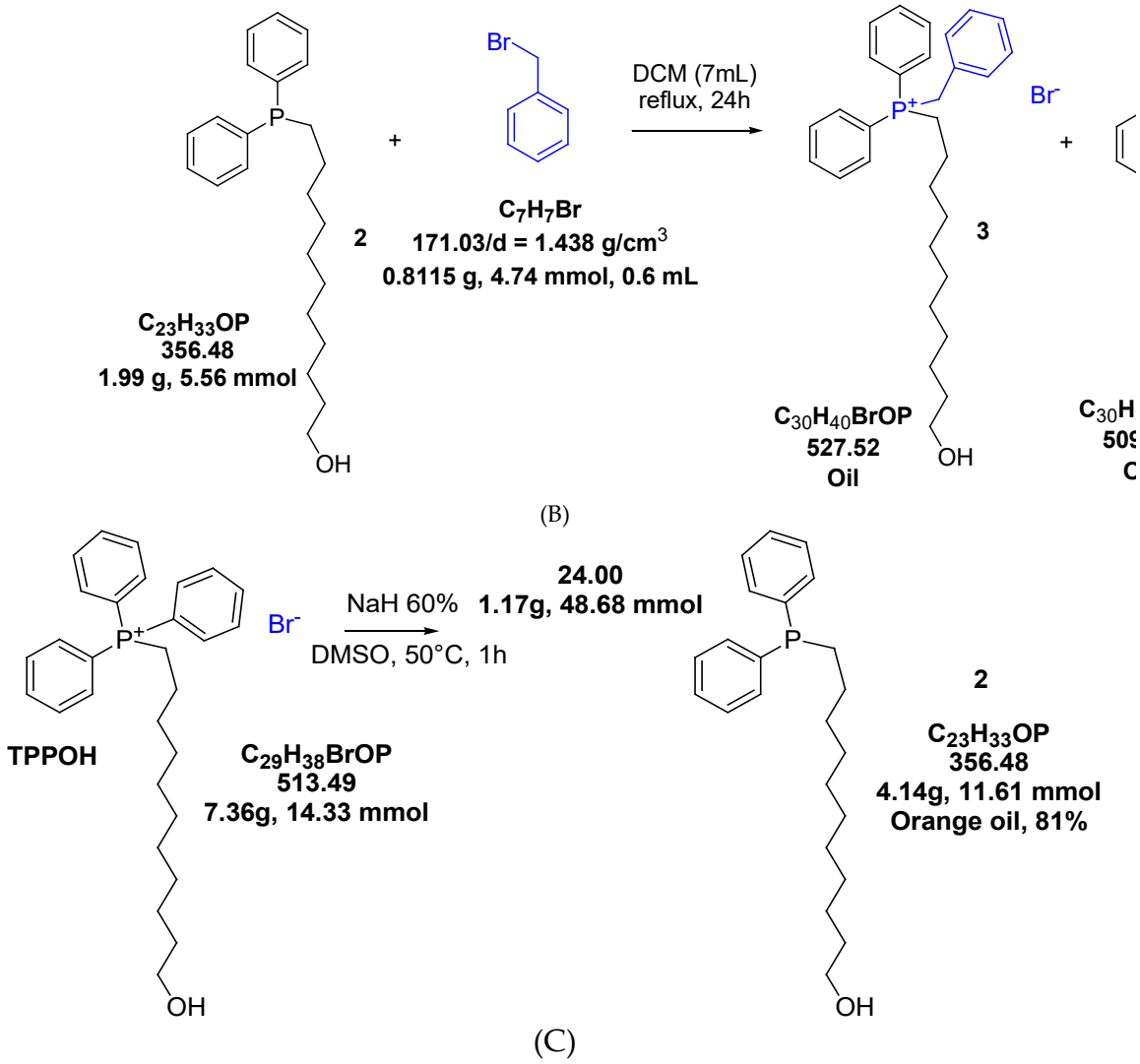

Scheme 1. (A) Synthetic procedure to prepare compound **1** [58]; (B) synthetic procedure to achieve compounds **3** and **4**; (C) synthetic procedure followed to prepare precursor **2**. DCM = dichloromethane.

As observable in Chart 1 and Scheme 1B, compounds **3** and **4** were different because, **3** has a hydroxyl on carbon atom C11, while **4** contains a C10-C11 double bond. The synthesis and full characterization of **1**-**4** have been described in our recent work[18]. Chemometric-assisted ATR-FTIR, ^{1}H, ^{13}C, ^{31}P NMR and UV-Vis spectroscopies were used to confirm their structure and evaluated their level of purity[18]. The interpretation of NMR spectra and peaks assignation was carried out with the help of literature data [59] and of ChemNMR H-1 Estimation tool associated with ChemDraw Ultra 7.0 software[18]. Copies of NMR spectra are available in Section S1 of Supplementary Materials file associated to this study (Figure S1.1-S1.16), while those of ATR-FTIR ones are consultable in Section S2 (Figure S2.1-S2.4). Conversely Figure S3.1. in Section S3 shows the copy of UV-Vis spectra of **1**-**4**.

2.2. Morphology Compounds 1-4 in Methanol and Water by Optical Microscopy

Optical microscopy analyses were used to investigate the morphology of **1**-**4** in water suspension and methanol (MeOH) solution and to choose samples worthy of more in deep and reliable investigation by dynamic light scattering (DLS) analyses.

2.3. Dynamic Ligh Scattering (DLS) Analyses of 2, 3 and 4

The hydrodynamic size (diameter) (Z-AVE, nm) and polydispersity index (PDI) of **2**, **3** and **4**, which demonstrated in optical analyses to form micro-vesicles both in water suspension and in MeOH solution (Supplementary Materials file, Section S4, Figure S4.1)[18] were determined by DLS

 doi:10.20944/preprints202603.0534.v1

analysis to assess the actual dimensions of particles and how much their distribution could be uniform. Three measurements, made of ten runs (called records in DLS images) each one, were carried out, and results of records acquired by number (%) were reported in the images (Figure 1a, c, e), to enhance the intensity of the peaks of the most represented dimensional family (≅ 99%) respect to that of other dimensional families (< 1%). Specifically, reported Z-AVE (nm) is the mean ± S.D. of the records acquired at the highest kcps value, which is a measure of concentration of sample. Similarly, PDI related to reported record was provided. Additionally, zeta-potential (ζ-p) measurements for all samples (**1**-**4**) were carried out on their water dispersions to determine their surface charge. Provided ζ-p values were obtained by three measurements, made of 12 runs each one, and was reported as mean ζ-p ± S.D. As above anticipated, size-related images evidenced the presence of more than one-dimensional family for all samples. Two-dimensional families were observed for samples **2** and **3** and the less representative (< 1% by number) was made of micrometres aggregates. Three ones were observed for sample **4**, where the less representative (4.5% by intensity) was made of very large micrometres particles, while the intermediate one (15.3% by intensity) was made of nanoparticles slightly smaller than those of the most representative one (80.2% by intensity). This multi-family distribution was mainly visible in analyses acquired by intensity (%). A representative image of such acquisitions was reported only for compound **4** in Section S5, Supplementary Materials (Figure S5.1). Figure S5.1 shows three DLS records acquired by intensity, where three major peaks were visible, but data for only two of them have been reported. About these most intense two peaks (92.6 and 80.2% by intensity), size was 1105±252.4 and 810.0±196.0 nm (kcps = 20.2 and 20.5), respectively. Associated to these peaks, smaller ones (5.2 and 15.3% by intensity) were detected having a smaller size of 152.0±20.2 and 232.7±37.3 nm, respectively. Coupled to these peaks, much smaller three peaks were also detected at high dimensions. These two new peaks had intensity 2.3 and 4.5% respectively, and a larger size of 5.560±0.043 × 10^{-3}. Collectively, on the base of these data the Z-AVE of particles of **4** from two runs was 1.596±0.156 μm, while their PDI was 0.7365±0.3726. Conversely, Figure S5.2 and S5.3 (Supplementary Materials) show the images of the three and two DLS acquisitions by number (%) made on **2** and **3** respectively. Concerning **2**, two peaks at 604.9±218.2 nm (99.2%, kcps = 12.7) and one more intense peak (99.4%) at 805.4±239 (nm kcps = 7.2), were observable. Additionally, three other very small peaks (0.6-0.8% by number), belonging to very large particles of about 5.0±0.788 and 5.5±0.627μm, were visible. Each acquisition provided a weighted average (based on the numerosity of particles) Z-AVE with an associate PDI (Figure S5.2) of particles of **2**. Collectively, on the base of these data the Z-AVE of particles of **2** from three acquisitions was 1.033±0.231 μm, while their PDI was 0.414±0.038. Analogously, Figure S5.3 shows the representative image of only two DLS acquisitions by number (%) made on **3**, where two intense peaks (99.4 and 99.1% by numbers) at 156.9±54.4 and at 178.2±53.7 nm (kcps = 14.2 and 11.3, respectively), related to the most represented family are observable. Associated to these peaks, very smaller ones (0.6 and 0.9% by numbers) were detectable at 1.163±0.517 μm and 962.4±780.2 nm, related to the larger dimensional family. Collectively, on the base of these data the Z-AVE of particles of **3** from two acquisition by number (%) was 332.6±16.3 nm, while their PDI was 0.496±0.082. Anyway, by considering only the acquisition by number (%) recorded at the highest kcps and the most represented dimension families (> 99% for 2, 3 and > 91% for 4), Z-AVE of particles of **2** , 3 and 4 were 604.9±218.2, 156.9±54.4 and 156.9±54.4 nm, while their PDI was 0.370, 0.438 and 0.438 (Table 1).

Table 1. Average hydrodynamic diameter (Z-AVE, nm) obtained by records acquired by number (%) at the highest kcps and average zeta-potential (ζ-p, mV) obtained by records acquired at the highest kcps.

Sample	Z-Ave (nm), kcps	ζ-p (mV), kcps
1	N.D.	38.10±6.15, 143.2.1
2	604.9±218.2, 12.7	4.19±3.26, 1.1
3	156.9±54.4, 14.2	15.7±5.07, 31.9
4	140.4±22.9, 24.2	13.4±7.63, 93.8

 doi:10.20944/preprints202603.0534.v1

N.D. = Not determined.

Single o two acquisitions by numbers (%), which enhanced the highness of peaks of the most representative family (~99%), while flattened that of less representative ones (< 1%) were reported here (Figure 1a, c, e). Three representative acquisitions out of 12 runs were instead reported for their ζ-p (mV) distribution (Figure 1b, d, f).

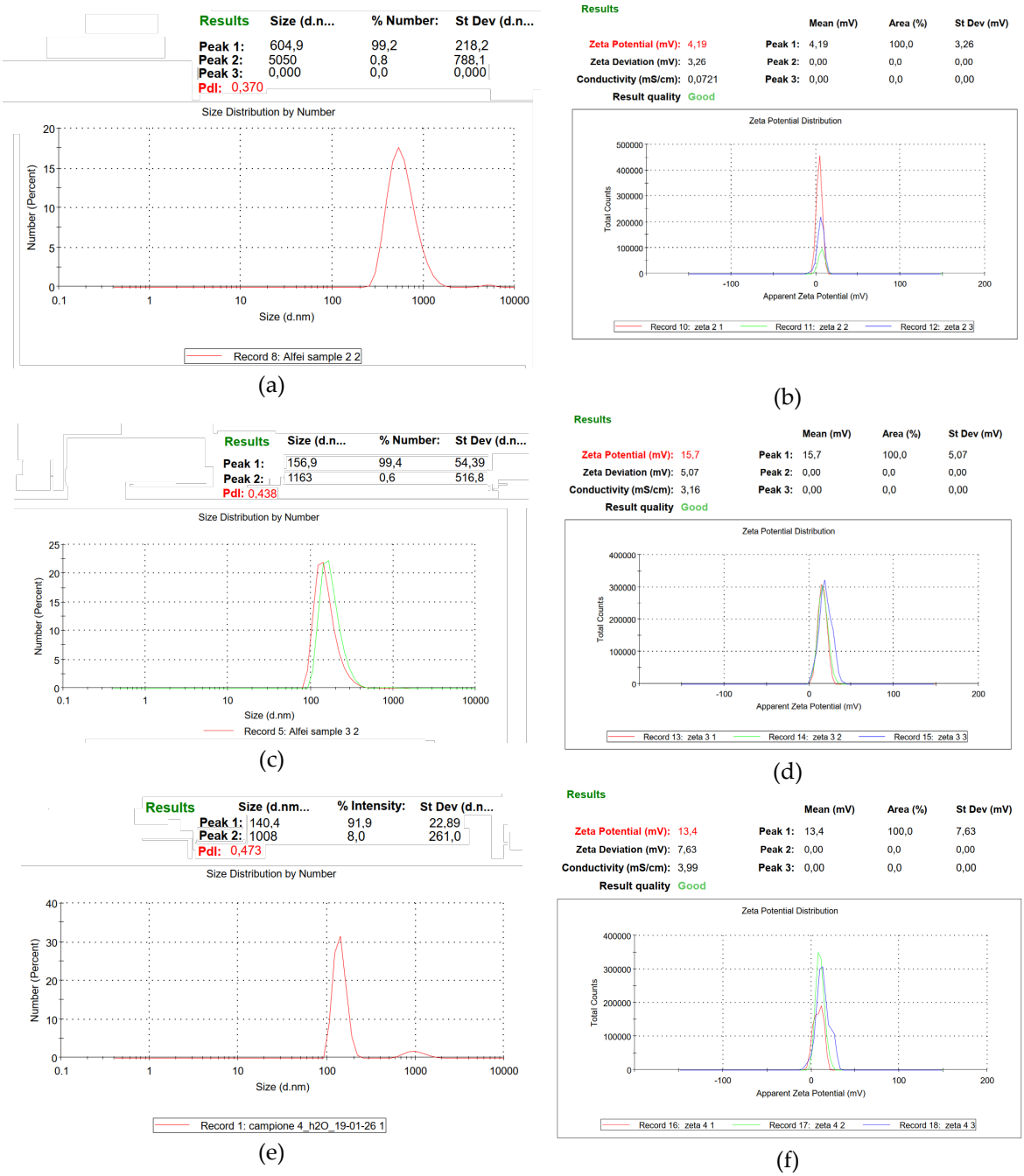

Figure 1. (a, c, d) Average hydrodynamic diameter (Z-AVE, nm) distributions, obtained by records acquired by number (%) at the highest kcps. (b, d, f) Average zeta-potential (ζ-p, mV) distributions obtained by the three records.

The following Figure 2 shows the ζ-p distribution of three runs acquired at 25 °C and 143.3 kcps (due to its higher solubility respect to other compounds) of **1** in water.

 doi:10.20944/preprints202603.0534.v1

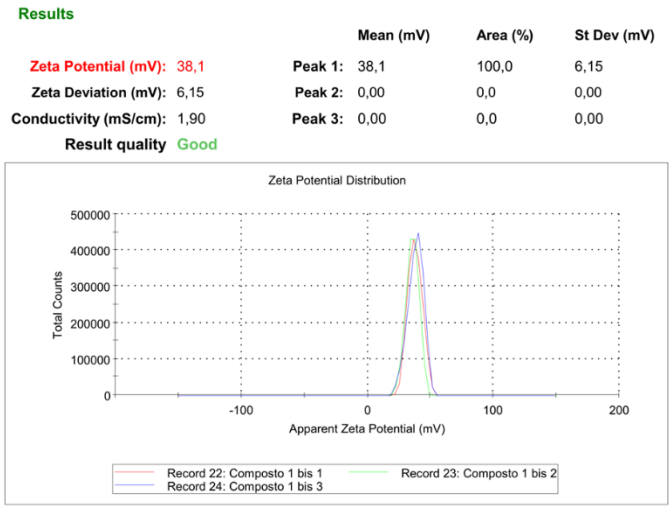

Figure 2. Three records of the Zeta-potential (ζ-p, mV) distributions of **1** (143.3 kcps).

The phenomenon of multi-dimensional families has been previously reported for a bola amphiphilic QPS molecule [27]. It is reported that the detected micrometres particles probably consisted of insoluble large aggregates[60], whose formation was promoted by the scarce solubility of all compounds in water, especially of **2**, which was the main factor that hindered the reading of reliable MICs in early microbiologic experiments. Nonetheless, filtration to remove larger aggregates was not possible, since such an operation would have too much lowered the number of kcps, invalidating the analysis. The variety of dimensional families of vesicles found in DLS analysis could be a sign of a phenomenon like the well-known "bolalipid's polymorphism", which justify also the presence of families of nanoparticles smaller than those of the most representative one [60]. Concerning surface charge, while all compounds demonstrated a positive ζ-p, but not high for **2**, **3** and **4** (ζ-p = +4.2, +15.7 and +13.4 mV), being the highest that of compound **3** (Figure 1b, d, f), compound **1** showed a ζ-p value decisively high of 38.1 mV (Figure 2). A positive ζ-p is a key factor for the antibacterial activity of cationic nanoparticles and nano vesicles as **3** and **4**, as well as of cationic salts as **1**, despite its incapability to form NPs due to its not amphiphilic structure. In this regard, we are confident that, if made more soluble upon proper chemical modifications, to improve kcps in solution and to render possible the reading of reliable MICs, compounds **3** and **4**, but perhaps also **2**, despite apparently not cationic, could demonstrate even higher positive ζ-p and therefore a certain antibacterial effect. In fact, bacterial surfaces, like surface of cancer cells, are generally negatively charged, due to the presence of lipopolysaccharides, teichoic acids, and anionic phospholipids. Consequently, systems with a positive surface charge can exhibit a strong electrostatic attraction toward the bacterial membrane as well as that of cancer cells, which increases contact and adhesion [21–23]. This interaction can lead to surface charge neutralization, destabilization of the lipid bilayer, and increased membrane permeability, resulting in loss of cell integrity and bacterial, as well as cancer cells death. It has been reported that, a markedly positive ζ-p is associated with strong anticancer properties, as well as increased and broader spectrum antibacterial efficacy, even at lower concentrations [53,61,62]. There is evidence, that nanovesicles with significantly high positive ζ-p (+18.33 mV), but < +30 mV, maintained a high anticancer effect and a broad antibacterial activity, but exerted only bacteriostatic effects, being not bactericidal as other compounds which demonstrated positive ζ-p up to +49.8 and +57.6 mV [27,53,61,62]. Additionally, high positive values of ζ-p can help reduce biofilm formation [63], making these systems particularly attractive also for antimicrobial coatings and targeted drug delivery [21–23].

On these considerations, due to the high positive ζ-p = +38.1 mV measured for **1** it was rationally thought that it could possess broad spectrum (not experimentally confirmed), bactericidal and antibiofilm properties (experimentally confirmed).

 doi:10.20944/preprints202603.0534.v1

2.4. Antibacterial Properties of QPSs 1-4

2.4.1. In Vitro Antibacterial Activity of Compounds 1-4 by Determining MIC Values (MICs)

Roadmap Followed to Assess the Antibacterial Effects of Compounds **1**-**4**

Experiments were conducted to evaluate the antibacterial behaviour of the synthesized compounds **1**-**4** starting from determining their minimum inhibitory concentrations (MICs) on a narrow selection of multidrug resistant (MDR) Gram-positive and Gram-negative clinical isolates and following the roadmap schematized in Figure 3.

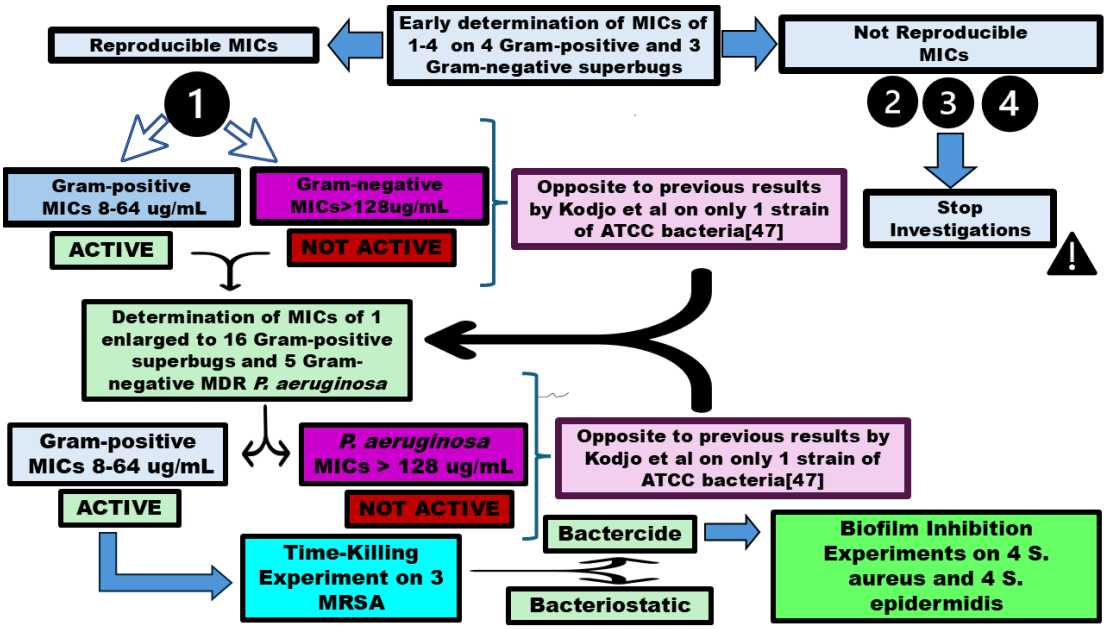

Figure 3. Roadmap followed to microbiologically evaluate QPSs **1**-**4**.

As above-mentioned, MICs were first determined on a narrow selection of four Gram-positive and three Gram-negative MDR species. The impossibility to read reliable MICs for compounds **2**, **3** and **4**, due to their poor solubility was established, and such compounds were not further considered. Conversely, promising MICs for **1** were observed on MDR Gram-positive clinical isolates teste, while MICs > 128 μg/mL, retained by us the threshold for antibacterial activity, were observed on Gram-negative species. Since our findings were in contrast and opposite to previous reports by Kodjo et al [19]. investigations were enlarged to more strains of the same Gram-positive species tested in early experiments. Additionally, five MDR *P. aeruginosa* clinical isolates were tested, to confirm or confute the negative results obtained by us in the early screening, thus definitely establishing the actual antibacterial effects of **1**. Then, to widen the antibacterial investigation made by Kodjo et al on **1** [19], never performed time kill experiments were carried out with **1** on selected MRSA, to assess if it could be bactericide. Once established its bactericidal activity, accurate biofilm inhibition tests were carried out with **1**, using the four MRSA and four MRSE strongest biofilm-producers of our collection. All bacteria used in this study were clinical isolates that had developed resistance to at least one or two antibiotics, including also ESKAPE species.

Early Experiments and Findings

The results from these screening experiments have been summarized in Table 2.

Table 2. MICs of compounds **1**-**4** against MDR clinical isolates of a narrow selection of Gram-positive and Gram-negative species obtained from experiments conducted at least in triplicate. The modal value was considered as MIC, and results have been reported expressed as μg/mL.

 doi:10.20944/preprints202603.0534.v1

Strains	1 (433.3)[1]	2 (356.5)[1]	3 (527.5)[1]	4 (509.5)[1]	V/T	OXA
			MIC μg/mL			
S. aureus ATCC 29213 MSSA	16	N.L.	N.L.	N.L.	0.5(V)	0.5
S. aureus B MRSA	8	N.L.	N.L.	N.L.	0.25(V)	512
S. epidermidis 22 MRSE	16	N.L.	N.L.	N.L.	0.5(V)	128
E. faecalis 1VRE, *	64	N.L.	N.L.	N.L.	256(V); 64(T)	N.R.
E. faecium 152 VRE, *	64	N.L.	N.L.	N.L.	128(V); 64(T)	N.R.
P. aeruginosa 259 **, CF, CR	> 128	N.L.	N.L.	N.L.	N.R.	128
E. coli **, ***	> 128	N.L.	N.L.	N.L.	N.R.	128
K. pneumoniae **, ***	> 128	N.L.	N.L.	N.L.	N.R.	256

[1] MW of compounds; MSSA = methicillin-sensitive; VRE = vancomycin-resistant enterococci; MRSA = methicillin resistant *S. aureus*; MRSE = methicillin resistant *S. epidermidis*; * denotes resistance also to teicoplanin; ** indicates resistance to carbapenems; CF= from patients with cystic fibrosis; CR = resistant to colistin; *** indicates resistance to carbapenems by producing class A *K. pneumoniae* carbapenemase ; N.L. = not legible; V = vancomycin; T = teicoplanin; OXA = oxacillin; N.R. = not reported.

Compounds **2**, **3** and **4** provided not legible MICs, due to their poor solubility, and were considered not suitable for further investigations, in this study, if not properly modified. For the moment, the actual activity of **2**, **3** and **4** remains a mystery. Terekhova et al. demonstrated the antibacterial activity against Gram-positive *S. aureus* depending on the length and structure of their alkyl chain, of ten diphenyl alkyl hydroxybenzyl phosphonium chlorides, having structures like those of **3** and **4** [43]. Surely, the presence of the hydroxyl groups, augmenting the solubility of compounds by Terekhova et al, was determinant for rendering authors capable to read MICs of such compounds, thus observing their significant antibacterial effects [64,65]. The most active molecules of Terekhova et al were compounds having C-10 (as **2**, **3** and **4**), C-12 and C-14 alkyl chains. They demonstrated very low MICs against clinically isolated *S. aureus* with resistance to amoxicillin and ciprofloxacin (SA1) or amoxicillin only (SA2) [43]. Specifically, MICs = 4 (SA1 and SA2), 1 (SA1), 2 (SA2) and 4 (SA1 and SA2) μg/mL were reported, for leading compounds. These findings evidence the importance of reevaluating **2**, **3** and **4** before their definitive rejection which, because, being nano dimensioned (605, 157 and 140 nm), are morphologically suitable for clinical uses and having positive surface charges and anticancer properties (**3** and **4**) could exert also antibacterial effects. Future structurally modifications of their structure, by strategic insertions of hydroxyls or doubling the cationic heads, could help in improving their solubility, to be capable to read reliable MICs. MICs of **1** were instead very interesting.

By the early investigations reported in Table 2, **1** was not active against *P. aeruginosa*, exhibiting MIC > 128 μg/mL, while was active against MRSA and VRE *E faecalis* (MICs = 16-32 and 64 μg/mL). Additionally, compound **1** was active also against MRSE and VRE *E. faecium* (MICs = 16 and 64 μg/mL).

These observations prompted us to confirm **1** antimicrobial behaviour against an enlarged population of Gram-positive clinical isolates and Gram-negative *P. aeruginosa*.

Enlarged Experiments and Results

 doi:10.20944/preprints202603.0534.v1

Compound **1** was tested against additional Gram-positive isolates of *Staphylococcus* and *Enterococcus* species for a total of 4 different MDR clinical isolates for each species (16 strains), and against other MDR *P. aeruginosa* strains for a total of 5 clinical isolates (Table 3).

Table 3. MICs of **1** against 16 MDR clinical isolates of Gram-positive species and 5 *P. aeruginosa* obtained from experiments conducted at least in triplicate. The modal value has been reported expressed as μg/mL.

Compounds	**1** (433.3) [1]	**oxacillin**	**vancomycin/teicoplanin**
Gram-positive Strains	**MIC (μg/mL)**	**MIC (μg/mL)**	**MIC (μg/mL)**
S. aureus 18 MRSA	32	512	0.5(V)
S. aureus ATCC 29213 MSSA	32	128	0.5(V)
S. aureus 189 MRSA	16	0.5	0.5(V)
S. aureus B MRSA	8	512	0.25(V)
S. epidermidis 22 MRSE	16	128	0.5(V)
S. epidermidis 25 MRSE	64	256	0.5(V)
S. epidermidis 64 MRSE	64	128	0.5(V)
S. epidermidis 147 MRSE	64	64	1(V)
E. faecalis 1 VRE, *, **	64	N. R.	256(V); 64(T)
E. faecalis 439 VRE, *	64	N. R.	256(V); 64(T)
E. faecalis 365 VRE, *, **	64	N. R.	32(V) ;1(T)
E. faecalis 451 VRE, *	64	N. R.	128(V); 32(T)
E. faecium 152 VRE, *, **	64	N. R.	128(V); 64(T)
E. faecium 183 VRE, *, **	64	N. R.	256(V); 64(T)
E. faecium 185 VRE, *, **	64	N. R.	256(V); 32(T)
E. faecium 364 VRE, *	64	N. R.	64(V); 005(T)
Gram-negative Strains	**MIC (μg/mL)**	**MIC (μg/mL)**	**MIC (μg/mL)**
P. aeruginosa 259 ***, CF, CR	> 128	> 128	N. R.
P. aeruginosa 229 ***, CF	> 128	> 128	N. R.
P. aeruginosa 247 ***	> 128	> 128	N. R.
P. aeruginosa 256 ***	> 128	> 128	N. R.
P. aeruginosa 268 ***	> 128	> 128	N. R.

[1] MW of compounds; MSSA = methicillin- (oxacillin) sensitive; VRE = vancomycin-resistant enterococci; MRSA = methicillin resistant *S. aureus*; MRSE = methicillin resistant *S. epidermidis*; * denotes resistance also to teicoplanin; ** denotes resistance also to linezolid; *** indicates resistance to carbapenems; CF= from patients with cystic fibrosis; CR = resistant to colistin; N.R. = not reported. All *P. aeruginosa* were MDR resistant; V= vancomycin; T = teicoplanin; N.R. = not reported.

Results in Table 3 confirmed the early finding in Table 2. Notably, behaviour of **1** against *S. aureus*, *E. faecium* and *P. aeruginosa* was completely different and opposite to that reported by Kodjo et al against ATCC strains of same species, while confirmed that reported by other authors[39,42,43,49,66]. MICs = 8-32 μg/mL against four strains of *S. aureus* (3 MRSA), MIC = 64 μg/mL against four VRE *E. faecalis* also resistant to teicoplanin and in some cases to linezolid, and MIC > 128 μg/mL against MDR *P. aeruginosa*, were observed. When QPS **1** was studied by Kodjo et al., as new benzyl containing QPS antibacterial weapon, authors found it active against the worrying Gram-negative *P. aeruginosa* (ATCC), while not active against Gram-negative *E. coli* (ATCC) and ATCC Gram-positive species, such as *S. aureus* and *E. faecalis* [19]. Specifically, Kodjo et al. found that their benzyl compounds, all having the unmodified or opportunely modified TPP group, were significantly active against *P. aeruginosa* and scarcely or completely not active on *S. aureus* and *E. faecalis* [19]. Among these miraculous molecules, two compounds, namely P-METHOXY and RABYL, very similar to **1**, were found inactive against *S. aureus* and *E. faecalis* and active on *P. aeruginosa* [19]. Specifically, MICs = 3.9, 500 and > 500 μg/mL were found for P-METHOXY against *P. aeruginosa, S. aureus* and *E. faecalis* respectively, and MICs = 2, 250 and >500 μg/mL were found for RABYL against

 doi:10.20944/preprints202603.0534.v1

same strains [19]. More incredible for us, the compound tested by Kodjo et al. identical to **1** was reported to have significant activity against *P. aeruginosa* (MICs = 31.3 μg/mL) and to be not active against *S. aureus* and *E. faecalis* (MICs = 250 and > 500 μg/mL). These findings were never previously reported by other authors for similar benzyl compounds [42,43,49,67] or compounds containing only one TPP group [26,68,69]. Usually, similar mono-cationic compounds were found active on Gram-positive species and not on Gram-negative ones. No of 10 benzyl compounds developed by Terekhova et al. was found active against Gram-negative strains [43], as instead reported by Kodjo et al. for **1** and other their benzyl QPSs [19]. At least, it is reported that two TPP-cationic heads are necessary to have activity against Gram negative species [27,68].

Also, other compounds, which are simply more complex versions of **1**, were in fact synthesized by Milenković et al and Galkina et al [42,49], and overall tested against Gram-positive *S. aureus*, *Bacillus Subtilis,* and *Micrococcus lysodeikticus*, as well as against Gram-negative *E. coli*, *Salmonella paratyphoid* B, and *P. aeruginosa*. Compounds were acyl hydrazone derivatives having a chloride anion (**1**-**4**, Milenković et al [49]) and a quaternary TPP QPSs having a 2,6-di-tert-butyl-4-methylphenol group and a bromine anion (**4**, Galkina et al [42]). Both authors ascertained the antibacterial activity of their compounds using the method of the inhibition zone. According to Galkina et al, the antimicrobial activity observed against Gram-negative species, such as *P. aeruginosa*, *E. coli* and *Salmonella paratyphoid B* were lower by 2.7, 2.7 and 2.4, respect to that observed against Gram-positive *S. aureus* [42]. Similarly, according to Milenković et al, compounds were not active against Gram-negative species, while were active against Gram-positive ones [49]. The same Galkina et al, ten years later, synthesized benzyl QPSs analogous of their compound **4**, having two diphenyl benzyl cationic heads linked by a C2, C3, or C6-alkyl chain and tested them on *E. coli, Bacillus cereus, P. aeruginosa* and *S. aureus* [70]. Despite, these QPSs possessed two phosphonium cations, were only slightly more active against *E. coli* and *P. aeruginosa*. Specifically, the best compound **3b** was anyway more active against Gram-positive *S. aureus* by 1.3 and 2.4-folds, respect to the activity observed against *E. coli* and *P. aeruginosa*, respectively [70]. The low activity of these new *bis*-QPSs respect to that of another reported compound [27], could depend on the absence of the TPP group and on the presence of too short alkyl chain of 2-6 carbon atoms, while is know that the best activity required a chain of 10-14 carbon atoms[60]. On these considerations, we are confident that ours double-checked results are correct, thus establishing that **1** is active only against Gram-positive bacterial species, as observed by other authors for similar compounds[43,49], but not against Gram-negative isolates. Compound **1** was found inactive also against other clinically relevant representatives of Gram-negative specie such as Enterobacteriaceae. Specifically**, 1** was inactive against *E. coli* (MIC > 128 μg/mL), as reported also by Kodjo et al. (MIC > 500 μg/mL) and *K. pneumoniae* (MIC ≥ 128 μg/mL), not tested by Kodjo et. [19]. Despite inactivity of **1** against Gram-negative superbugs was confirmed, its antibacterial effects against all Gram-positive MDR clinical isolates used here are of paramount importance, since some of them belong to ESKAPE bacteria group [71], currently considered a major therapeutic challenge despite the introduction of several new antibiotics and antibiotic adjuvants, such as novel β-lactamase inhibitors[71].

About Antibacterial Properties of TPP-salts Previously Reported

Also, compared to the antibacterial activity demonstrated by TPP-salts conjugated to ciprofloxacin by ester-linkages reported by Kang et al against VRE, MRSA and VISA, that of **1** against VRE also resistant to linezolid and MRSA also resistant to teicoplanin was higher by 4 and 2-16-folds [72].The antibacterial activity of **1** against MRSE, MRSA and *E. faecium* VRE also resistant to teicoplanin and linezolid, was comparable to that of same TAPILs bromides and chlorides against standard strains from the National Collection of Type Cultures (NCTC) London and ATCC, including *S. epidermidis*, *S. aureus* and *E. faecium*. TAPILs were not found active against *P. aeruginosa* [48] as **1**. Cieniecka-Rosłonkiewicz et al. evidenced that different anions could substantially affect the antibacterial activity of cationic salt, and in this regard, some TAPILs with chlorine counterions, showed MICs significantly higher than those of **1** and up to 125 μg/mL (compound **2g**) against NCTC *S. aureus* and ATCC *E. faecium* [48]. Anyway, despite MICs and MBCs of some TAPILs against

 doi:10.20944/preprints202603.0534.v1

standard strains of *S. epidermidis* and *E. faecium* were very low, they were in almost all cases higher than those of benzalkonium chloride (BAC) [48]. BAC is a commercially available mixture of quaternary ammonium salt (QAS), having an average molecular weight of 368, known to be a potent biocide, which acts mainly a-specifically, disrupting the bacterial cell membranes, denaturing proteins, and damaging the essential metabolic enzymes, leading to bacterial death[73,74]. Anyway, frequently, bacteria demonstrate heterogeneous susceptibility to BAC, due to both genetic factors (presence of qac efflux genes, 80%) and physiological states (planktonic vs. biofilm, stationary vs. exponential phase), as well as several other factors [75]. BAC has been reported to have MICs = 4 μg/mL against NCTC 13143 *S. aureus*[76], MICs = 2-10 or 5/5.1 μg/mL against MRSA, depending on different studies [77–79]. Cieniecka-Rosłonkiewicz reported MICs equal to 0.5, 1.0 and 2.0 μg/mL against standard strains of *S. epidermidis, S. aureus* and *E. faecium*[48]. Rahami et al reported that different gene mutations between different HA-MRSA strains affected the resistance of HA-MRSA to BAC [80]. Previous tests against HA-MRSA, isolated from various hospitals in Rome (Italy), resulted in BAC having different MICs on the various HA-MRSA strains tested (2 μg/mL, 4 μg/mL, 8 μg/mL, and 16 μg/mL) [80]. Results reported in the research by Rahami et al conducted to established MICs of BAC against HA-MRSA by colony counting method, suggested that MIC of BAC determined where no growth of bacterial was observed was 5 μg/mL[80]. Also, Akimitsu et al and Rahmi et al reported that MIC of BAC against parent MRSA (5 μg/mL), and those of 5 MRSA strains, which muted under administration of 5 μg/mL BAC (10 μg/mL), increased by 7.1-14.2-times respect MICs against MSSA [81]. Collectively, reported MBCs for BAC against *S. aureus*, are different depending on the different studies, different conditions for determinations and the *S. aureus* type. Worthing et al reported MBC values against MRSA in the range 33.7-135 μg/mL in presence of bovine serum albumin (BSA), while they ranged from 2.1 to 16.9 μg/mL in absence of BSA [77]. Cieniecka-Rosłonkiewicz et al reported MBCs = 8 μg/mL against *S. aureus* NCTC 4163 [48]. On all these reports, while BAC is less potent than the previously reported BPPB, it is strongly more potent than **1** [27]. On the other hand, BAC is toxic for the environment and genotoxic at 1 μg/mL towards rats' hepatocytes and human lymphocytes [82], thus having SIs in the range 0.06-0.5, which limits its use as topic or environmental detergent or disinfectant. In this regard, selectivity of **1** for MRSA respect to eukaryotic cell lines (human keratinocytes HaCaT and murine fibroblasts 3T3 cells), as well as red blood cells (RBCs) was extremely higher than that of BAC, allowing for SIs in the range 15.7-62.6, 47.4-189.5 and 1.7-6.6, respectively. The toxicity of **1** is extremely lower than that of BAC, thus establishing its potential suitability for clinical applications. Additionally, despite the biocide mechanism of BAC consists of general multiple and non-specific target sites against bacteria, thus suggesting that bacterial resistance might be difficult to emerge, when the biocide is used at a high concentration, generally above the MIC value to have complete extermination of bacteria, this holds mostly true [75]. In fact, the emergence of bacteria resistance upon the use of BAC has been widely reported in vitro and is perceived to present as a high risk[75].

2.4.2. Structure Activity Relationships (SAR)

The structure of **1** presents four phenyl rings, three of which directly linked to phosphor atom and the fourth linked to phosphor atom by a unique methylene, thus being strongly hindered (Chart 1). Conversely, **3** and **4**, having only three rings, of which only two directly linked to phosphorous atom and an alkyl chain, are less hindered. Therefore, the cationic phosphor atoms in compounds **3** and **4** should have been more exposed than in **1** and possibly more likely to attract detrimentally, bacteria negatively charged envelop and inhibit them (Chart 1). On these observations, a major activity for compounds **3** and **4** than for **1**, could be forecasted, which for the moment remains a mystery due to their poor solubility. Anyway, it has to be considered that phosphonium salts serve as Brønsted acids, with phosphonium ylides acting as their conjugate bases. While phosphonium salts can undergo deprotonation, the ylide can be protonated by an acid, leading to the regeneration of the salt (Scheme 2)[83]. The two forms are in equilibrium, which can be moved towards the ylide form by promoting the deprotonation of the α carbon atom adjacent to the phosphorus atom.

 doi:10.20944/preprints202603.0534.v1

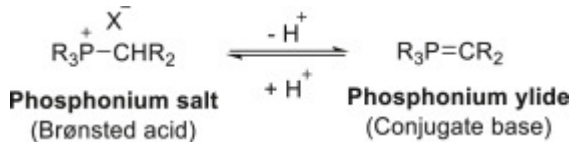

Scheme 2. Equilibrium between phosphonium salts (cationic) and their conjugate base (not cationic ylide).

While in the form of phosphonium salt phosphorous atom is cationic, so that capable to interact with bacterial walls causing damage and bacterial inhibition, in the ylide form the cationic charge is no longer present and electrostatic interactions are no longer possible. Collectively, when such equilibrium is possible and moved towards the not charged ylide forms, alkyl phosphonium salts have reduced possibilities to interact with bacteria by electrostatic attraction and reduction is proportional to the number of the possible ylide forms that phosphonium salts can have, based on their structure. As an example, in tetra alkyl phosphonium salts, up to four acid-base equilibria are possible, strongly reducing the number of molecules in the cationic status, respect to that of molecules in uncharged status (ylides) (ratio 1:4) and therefore lowering the possible interactions with bacteria (Scheme 3A).

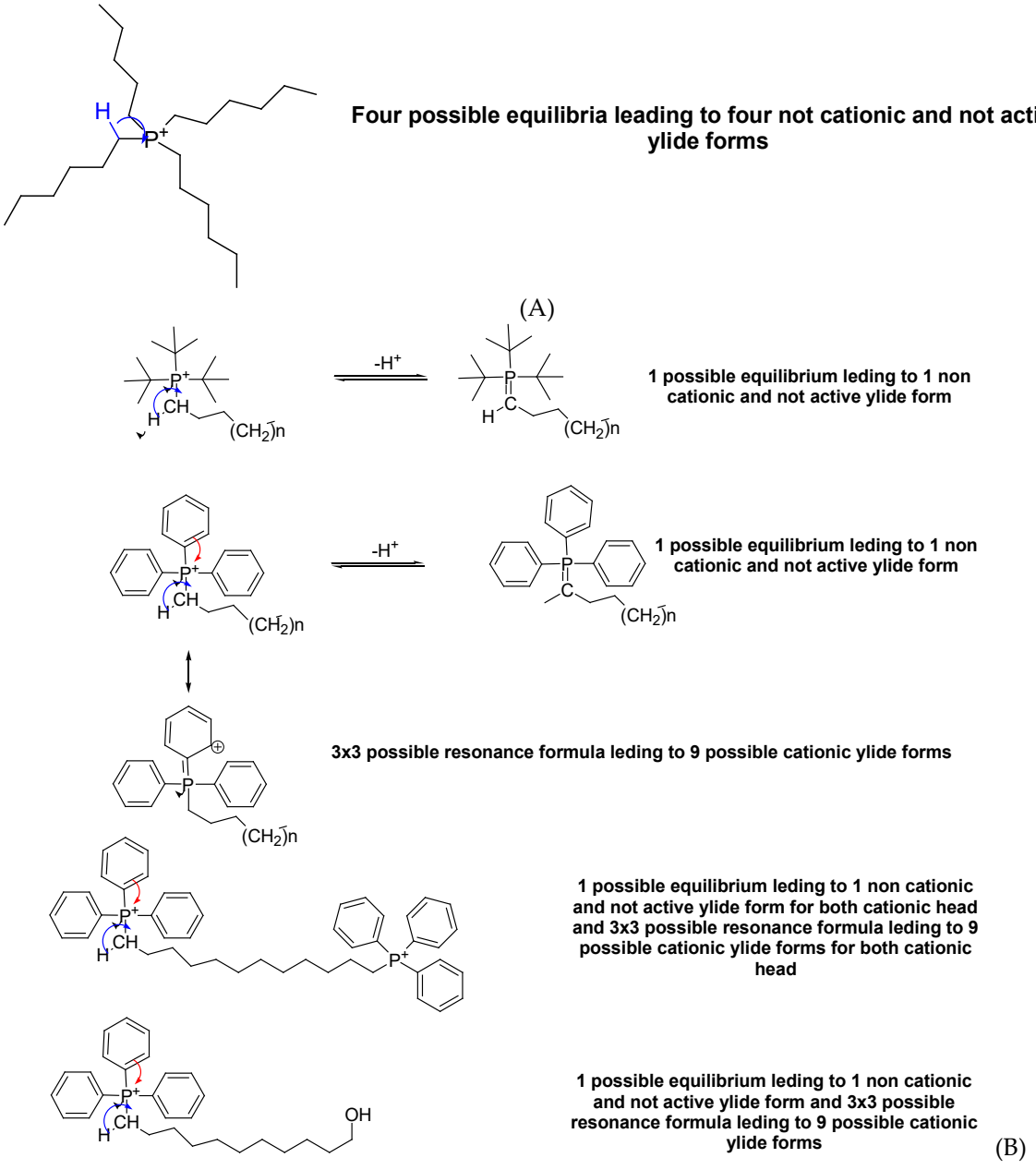

 doi:10.20944/preprints202603.0534.v1

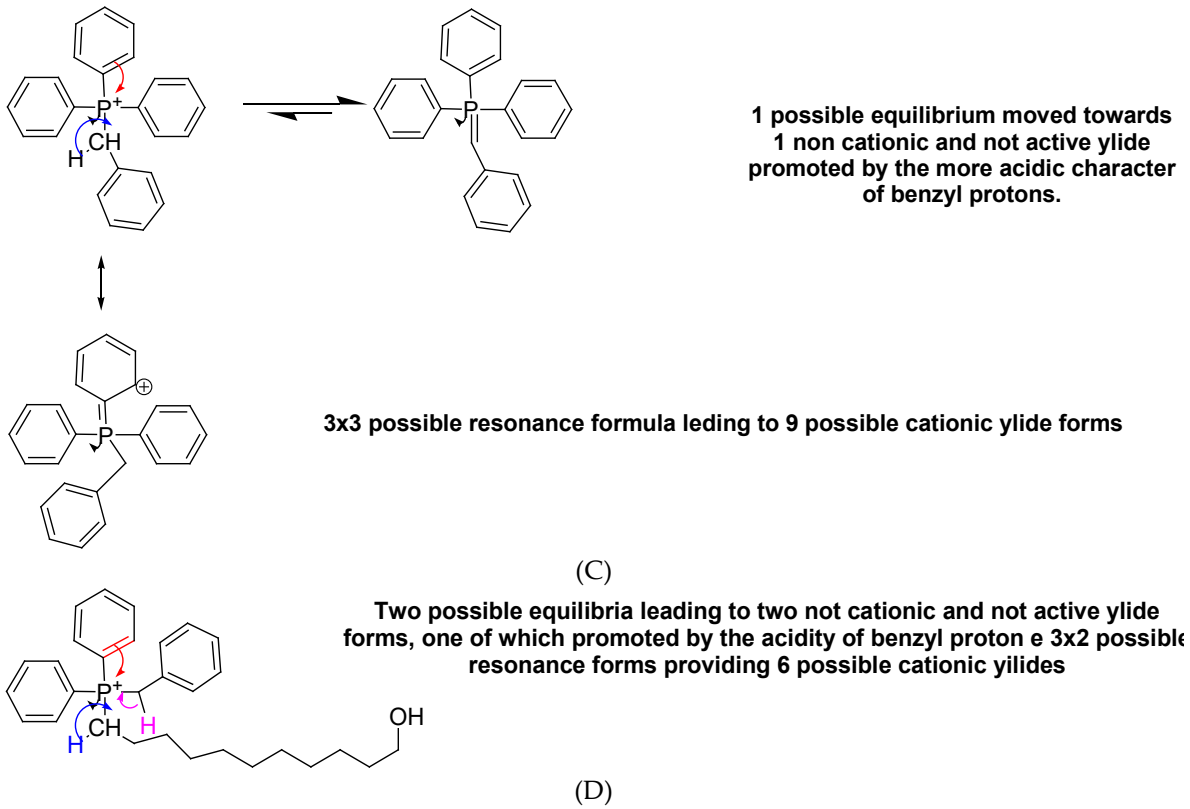

Scheme 3. Equilibria phosphonium salt/uncharged ylide and cationic ylide resonance formulas with cationic charge delocalized on the phenyl groups possible for soma QPSs.

When alkyl chains are progressively substituted with phenyl rings or tert-butyl groups directly linked to phosphor atom, the α protons dimmish as well as the possibilities of acid-base equilibria, and increasingly more cationic forms are present in solution, free to establish strong and detrimental electrostatic interactions with pathogens surface, thus augmenting their antibacterial effects. More phenyl rings or tert-butyl groups, up to a maximum of three, less the possibility to have acid-base equilibria leading to uncharged and inactive forms. These factors could justify the higher antibacterial activity of triphenyl and tri-tert-butyl alkyl phosphonium compounds, having only one alkyl chain, providing only one uncharged inactive ylide form [26,27,29,31–33] (Scheme 3B), versus that of tetra alkyl phosphonium salts [34] (Scheme 3A). Due to the possible existence of equilibrium in Scheme 2, despite the antibacterial activity of **3** and **4** remains for the moment unknown**,** a lower antibacterial potency than that observed for the triphenyl benzyl phosphonium salt **1**, having only one benzyl group, and not long alkyl chains, providing only an uncharged ylide form, could be though for them, having only two phenyl rings and benzyl alkyl groups allowing for two uncharged ylide forms (Scheme 3C and 3D). On suggestions found in Galkina et al., the insertion of hydroxyls on benzyl and/or phenyl groups could lead to improved solubility antibacterial effects due to the presence of phenols, known for its intrinsic antibacterial properties[42]. On the contrary, an enhanced antibacterial effect could be expected for compound **2** despite uncharged, because an opposite acid-base equilibrium leading to a cationic and active ylide (as already evidenced by the unexpected positive zeta potential) form the uncharged from is possible for this compound, whose cationic charge on phosphorous atom can easily delocalize on the phenyl ring in three for two (six) positions (Scheme 4).

 doi:10.20944/preprints202603.0534.v1

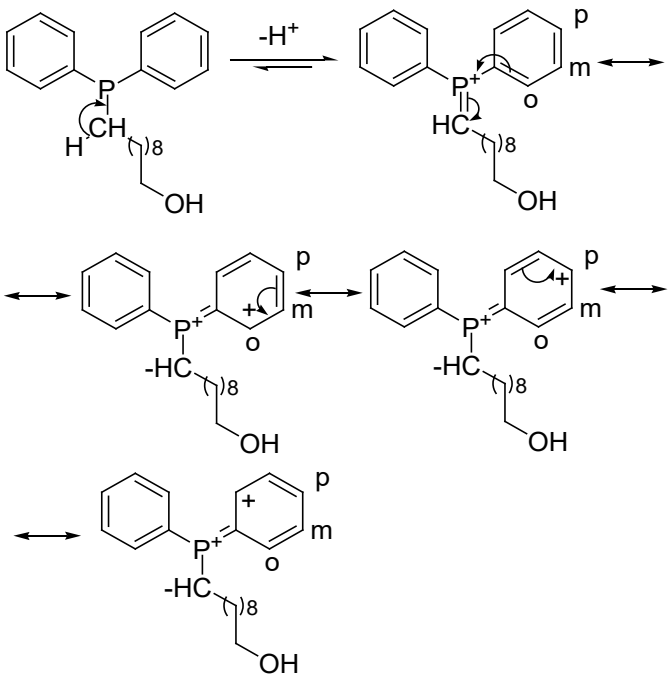

Scheme 4. Opposite acid-base equilibrium leading to a cationic and active ylide form the uncharged which is possible for compound **2**, and its three-resonance structure possible for each phenyl ring.

On the other hand, if three tertiary or phenyl groups linked directly to phosphorous atom are important to minimize the possibility of equilibria to not active forms, four is too much, due to the too high steric hindrance on cationic active charge. In fact, it has been reported that extremely hindered tetra phenyl phosphonium salts have been found completely inactive against Gram-negative *E. coli* [24]. Strong steric hindrance remains in **1** higher than that present in other TPP-compounds, tetra alkyl molecules and TAPIL2. This added to the presence of benzyl group, whose more acid proton atoms on methylene group, significantly move the acid-base equilibrium versus the uncharged ylide forms, justify their higher antibacterial behaviour respect to **1** [24,34,48]. Specifically, the presence of benzyl group in **1** could be the reason of its narrower spectrum of action and lower antibacterial activity respect to that of some triphenyl alkyl compounds previously reported [27,31,33], of some other tetra alkyl compounds [24,48] and of TAPIL2 reported by Banerjee et al., which showed to be active against both *E. coli* and *S. aureus*, at MICs = 3.9 μg/mL, despite their tetra alkyl composition [34]. Additionally, this structural aspect could justify the lower activity of **1** on Gram-positive species also respect to that of the triphenyl alkyl phosphonium reported by us [26]. On the other hand, the presence of phenyl rings directly linked to phosphorous atoms can improve the ratio charged phosphonium salt/uncharged ylides by the formation of C^{+}=C-C=P- cationic ylides as in compound **2**, with charge dislocated on each ring in three possible position, proportionally to the number of phenyl rings themselves (Scheme 4B, C and D). In this regard, despite less hindered, the simultaneous presence of an alkyl chain and a benzyl group in the structure of **3** and **4** shall lead to a limited cationic character, as already demonstrate by low zeta potential positive values. Collectively, the alkyl chain can have a double-face contribution on antibacterial properties of QPSs, while their length has a pivotal role [24,27]. While *N*-chloramine compounds with C3–C12 chains as linkers (compounds **3**–**5** in the study) demonstrated high biocidal efficacy after 10 min of contact, causing a 6.22 and 7.30 CFU log reduction in the initial inoculum of *E. coli* and *S. aureus*, respectively, compound **6** bearing a C12 chain was bactericidal after only 5 min of contact [95].

2.4.3. Time-Killing Curves

The time-kill kinetics assay is used to study the activity of an antimicrobial agent against a bacterial strain and is mainly used to determine the bactericidal or bacteriostatic activity of an agent

 doi:10.20944/preprints202603.0534.v1

over time [84]. For clarity, a time kill assay begins with preparing standardized microbial cultures. Cultures are grown to the logarithmic phase and adjusted to a consistent density, often around 10^5 to 10^6 colony-forming units (CFU) per millilitre, ensuring reliable results [85]. As for Clinical & Laboratory Standards Institute (CLSI) guidelines and other laboratory approved indications [84], bactericidal activity is then defined as greater than 3 $\log_{10}$-fold decrease in colony forming units (surviving bacteria), which is equivalent to 99.9% killing of the inoculum. A vehicle only control or/and only a growth control (as in our case) are included in the experiment as negative controls[84]. The log CFU/mL for all tested samples should be determined at time 0 and at subsequent time points up to 24 hours[62,86,87] since after a rapid decrease in the initial inoculum, frequently a rapid regrowth occurs in the following hours, due to an incomplete extermination of pathogens [88,89]. Anyway, it is difficult to find papers in which this indication is respected and frequently the showed analysis is stopped when > Log10 reduction is achieved (4-6 hours) without showing if any regrowth occurs in the subsequent hours to 24[72]. Other indications such as those included in the ASTM Standard Guide for Assessment of Antimicrobial Activity Using a Time-Kill Procedure. Method E2315–23, accredited by Spanish National Accreditation Entity (ENAC) can be used for antimicrobial agents that require variable/shorter time analysis (seconds/minutes), as antiseptics or as required by the clients of laboratory carrying out the analyses [90]. Time-kill data suggest a relationship between concentration, exposure time, and surviving fraction, which can be modelled probabilistically for editing infection control protocols[85]. To assess whether **1** was bactericidal or bacteriostatic, time-kill experiments were for the first time performed with **1**, at 4 × MICs for three selected strains (*S. aureus* ATCC 29213 and MRSA 18 at a final concentration of 128 μg/mL, while MRSA 189 at a final concentration of 64 μg/mL). As depicted in Figure 4, reporting the most representative curve obtained for MRSA strain 18, **1** demonstrated bactericidal effects as a decrease of > 3 $\log_{10}$ within 24 hours (equivalent to 99.9% killing of the inoculum) was reached.

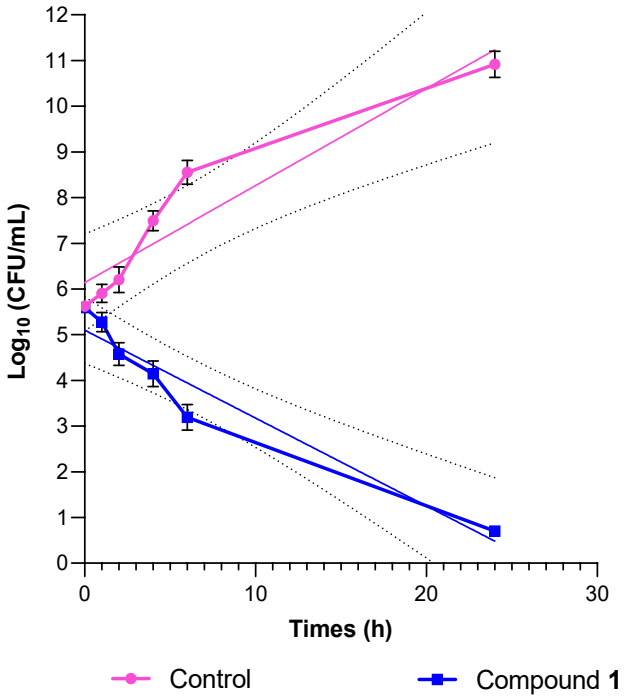

Figure 4. Time-killing curves obtained for control and for bacteria under treatment with **1** (at concentrations equal to 4 × MIC) against *S. aureus* 18 (blue lines with round indicators for control and pink lines with square indicators for bacteria under treatment with **1**), with linear tendency lines (thinner lines) whose equation related to that obtained for **1**, was used to calculate the time at which the > 3 $\log_{10}$ reduction in initial inoculum was reached. Punctuated curves indicate the confidence intervals (95%) around the regression lines.

 doi:10.20944/preprints202603.0534.v1

A similar trend was observed for MSSA ATCC 29213 (sensitive to oxacillin) and MRSA 189, despite their different pattern of resistance and concentrations (MRSA 189). In sight of these findings, it appears that, while the *bis* cationic QPS BPPB previously reported, when tested equally at 4 × MIC on same *S. aureus* 18 (MRSA) clinical isolate, resulted only bacteriostatic [27], **1** resulted bactericidal when tested in same conditions (4 × MIC). In fact, BPPB caused a decrease of < 3 log_{10} in the original cell number after 6 hours of exposure, followed by a slight increase and regrowth, which occurred during the next 24 hours. Conversely, a decrease of > 3 log (as required by CLSI) was reached within 11 hours, not followed by any regrowth during the subsequent 24 hours, was observed for **1**. Despite the MIC value of BPPB (0.25 μg/mL) against MRSA *S. aureus* 18 clinical isolate was remarkably minor than that of **1** (32 μg/mL) [27], the interesting aspect of the behaviour of **1** respect to that of BPPB regardless the concentrations used, consisted just in the absence of regrowth up to 24 hours, instead observed for bacteriostatic BPPB[27] and several other even short-time biocide cationic compounds [88,89], thus establishing a complete extermination of pathogens. Collectively, **1** was capable to complete exterminate MRSA and MSSA ATCC *S. aureus* without difference in the killing rate. Anyway, to better evaluate killing kinetics of **1**, a specific kinetic study was carried out, as detailed in the following section.

Kinetic Studies

To obtain valuable information on the pathways and mechanisms of bacterial growth in the control and bacterial dye under treatment with **1** over time, we carried out a kinetic study, fitting the time-killing curves in Figure 4 with two of the mainly used mathematical models previously reported[91–93]. Specifically, kinetic models of pseudo-first order (PFO) [Equation (1)], pseudo-second order (PSO) [Equation (2)], were studied.

$$\ln(GKe - GKt) = lnGKe - k1 \times t \quad (1)$$

$$\frac{t}{GKt} = \frac{1}{k2 \times GKe^2} + \frac{1}{GKe}t \quad (2)$$

where, *GKe* (Log_{10} (CFU/mL)) and *GKt* (Log_{10} (CFU/mL)) are the bacteria colonies at the end and at time *t* respectively, k_1 is the growth/killing kinetic constant of the PFO kinetic model (1/min), while k_2 that of the PSO kinetic model. Values of ln *(GKe-GKt)* and *t/GKt* were plotted vs. times. Dispersion graphs were obtained by using the already cited GraphPad software 8.0.1, and their linear regression lines were provided by the same software using the Ordinary Least Squares (OLS) method as well as their equations and related R^2 values (Figure 5). The coefficients of determination (R^2) of all the equations of the linear regressions obtained have been reported in Table 4 and were the parameters for determining the kinetic models that best fit data of time-killing (Figure 4) and the kinetic constants which governed the bacterial regrowth and killing.

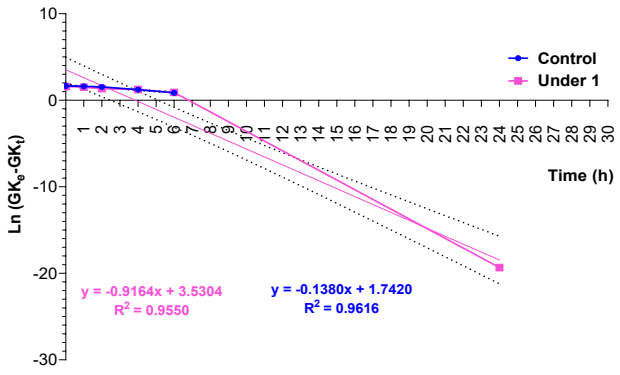

(A)

 doi:10.20944/preprints202603.0534.v1

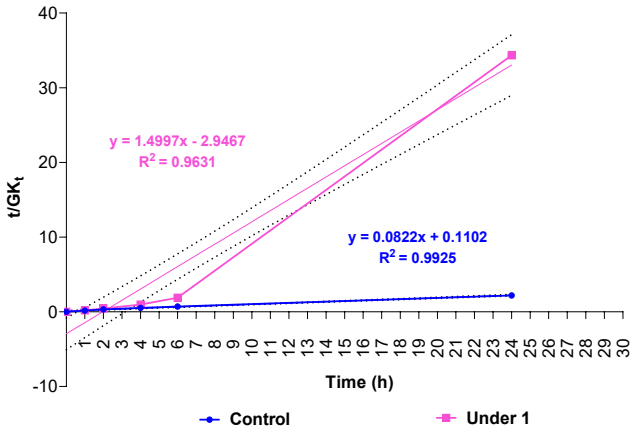

(B)

Figure 5. PFO and PSO models fitting the time-kill data (blue lines with round indicators for control and pink lines with square indicators for bacteria under treatment with **1**) with related linear regression lines (thinner lines). Punctuated curves indicate the confidence intervals (95%) around the regression lines.

Table 4. Values of coefficients of determinations (R^2) obtained for PFO and PSO kinetic models considered.

Kinetic Model	Control	1
PFO	0.9616	0.9550
PSO	**0.9925**	**0.9631**

The results in Table 4 showed that in both cases (control and **1**), the highest R^2 value was obtained with PSO model. Consequently, the kinetic behaviour of regrowth in the control and of killing by **1** followed the PSO kinetic model. The values of *GKe* and K^2 were computed using the values of the slopes and intercepts of the equations in Figure 5 and included in Table 5.

Table 5. Comparison of experimental number of bacterial colonies (in the control and under treatment with **1**) at the end of time-killing experiment with *GKe* form the kinetic model and values of K_2 provided by it.

Parameter	CTR *	CTR (EXP)	1	1 (EXP)
GKe (Log_{10}CFU/mL)	11.34 (*Ge*)	10.91	0.6668 (*Ke*)	0.6990
K_{PSO} **	0.0706	N.A.	0.5089	N.A.

GKe = Log_{10} (CFU/mL) at the end of time-killing process (*Ge* means bacteria grown in the control, while *Ke* means bacteria killed when treated with **1**); CTR = control; EXP = experimental; * Computed from the slopes of the equations in Figure 5; ** computed from the intercepts of equations in Figure 5.

The values of K_{PSO} established that killing of bacteria under treatment with **1** occurred much more rapidly (by 7.2-times) than their regrowth in the control. Additionally, the values of *Ge* and *Ke* perfectly agreed with experimental ones, as the minimal differences of 0.43 (3.8%) and 0.0322 (4.6%) confirmed. The potent biocide BAC was considered again for comparison, together with other TPP-salts, quaternary ammonium salts and ammonium polymers. Anyway, considering available time killing experiments for BAC administered at 100 μg/mL (an intermediate concentration between that used of **1** against MRSA 189 and 18), to MRSA, reported by Blondeau et al, BAC produced a > 5-log kill within 5 min and no regrowth up to 3 hours exposure[94]. In this regard, BAC is 6.4 million times more rapid in killing MRSA than **1** which reached > 5-log_{10} reduction was slowly reached at about 24 hours treatment, but regrowth was not observed (Figure 3). Without being critical to Blondeau et al, this possible behaviour of MRSA under treatment with BAC was not investigated by authors since the method used to evaluate the killing kinetics of BAC, does not respect the CSLI protocol. On the other hand, it was also reported that BAC at concentrations < 5-8 μg/mL, anyway at a toxic level for

 doi:10.20944/preprints202603.0534.v1

humans and environment (SI < 0.13-0.20) produces slow or incomplete killing, while at concentrations substantially above the MIC/MBC values, the killing rate increases, but persister subpopulations can cause a bimodal or multimodal time-kill curves [95], which were not observed with **1**. Rapid killing is achievable only at ≥ 10 × MIC, typically 150–300 μg/mL (SI = 0.006-0.003) for MRSA isolates. Sublethal exposure or inadequate contact time is very risky, since it can select for tolerant subpopulations, potentially facilitating cross-resistance to antibiotics used in humans. Therefore, despite MRSA was rapidly killed by BAC, with a 6-$\log_{10}$ reduction within ~1 h, but at genotoxic concentrations ≥ 150 μg/mL (SI < 0.006), 1 exterminated MRSA 18 and 189 (with > 5-$\log_{10}$ reduction) significantly less rapidly, but at lower no cytotoxic concentrations (128 and 64 μg/mL). Finally, kinetic killing constant (K_{PSO}), for reported TPP-compounds and quaternary ammonium salts (QASs), and two quaternary ammonium polymers (P5 and P7), whose time kill data best fitted the PSO mathematical model as in this case were compared with K_{PSO} of **1**. Specifically, K_{PSO} for reported TPP-salts were obtained fitting a PSO model to time-kill curve data obtained as an average curve of 3 studies were different TPP-salts with different killing behaviours were tested against MRSA with different patterns of resistance[32,72,96]. Similarly, it was made for reported QASs [97,98] (Table 6).

Table 6. Comparison of K_{PSO} values of **1** with those reported for other TPP-salts and QASs, as well as those of P7 and P5.

Compounds	Mathematical Model	K_{PSO}	Time (h)	Refs.
TPP- salts	PSO	0.5681	24	[32,72,96]
QASs		714.9	8	[97,98]
P7 (QAPs)		1.25	24	[53]
P5 (QAPs)		3.07	24	[62]
1		0.5089	24	This work

TPP = triphenyl phosphonium; QASs = quaternary ammonium salts; QAPs = quaternary ammonium polymers.

TPP-compounds are reported to be slower biocides (3–5 $\log_{10}$ CFU/mL reduction within 8–24 h) than QASs and QPSs because they act by a not classical membrane disruption, but bactericidal effect appears associated with mitochondria-like membrane targeting and possibly interference with bacterial energetics, analogous to their mito chondrial targeting in eukaryotic cells. On the contrary, QASs and QAPs exert a very rapid bactericidal effect, often within 1–4 h at concentrations ≥ MBC, due to a mechanism based on an immediate perturbation of the cytoplasmic membrane, a-specifically leading to membrane disruption via cationic–lipid interactions that compromise bacterial cell wall integrity. These salts show time-kill curves having a steep decline in CFU/mL within first 2–3 hours, despite a plateau or regrowth may occur if some bacteria survive sublethal exposure. Even if this possible behaviour is not observable in curves by Xiao as well as Saseendran et al [97,98], the possibility of its occurrence was confirmed in our study [53]. In this regard, **1** performance in killing MRSA was compared with that of reported TPP-compounds [32,72,96], while significantly lower than that of QAMSs and QAPs by 2.5, 6.0 and 1405-fold.

2.4.4. Antibiofilm Capacity of 1

The bacterial biofilm (BBF) is an organized community of bacteria that adheres to a living or non-living surface and surrounds itself with a polymeric extracellular matrix (EPS), composed primarily of polysaccharides, proteins, lipids, and extracellular DNA (eDNA)[99]. Collectively, BBF is a sort of three-dimensional "microbial city" where micro-organisms are numerous and cooperate with each other; protect each other with a physical and chemical barrier; and communicate through quorum sensing, a signalling system that coordinates collective behaviour[99]. Therefore, bacteria

 doi:10.20944/preprints202603.0534.v1

hindered in the biofilm and so well organized, are difficult to be or are no longer reachable by antibiotics which fail causing the widespread of severe or even intractable infections[99]. BFs are involved in over 60% of chronic wound infections, which can be colonized by a single or several bacterial species [100]. The major Gram-positive bacteria involved in BF formation are *S. aureus* and *S. epidermidis*[101,102]. The formation of BF by these bacteria represents the main virulence factor of the microorganisms, reducing the effectiveness of antibiotics by up to 1000 times and host immunity[103], thus promoting chronic, persistent and recurrent infections (bacteraemia and nosocomial sepsis, endocarditis (*S. aureus*), neonatal infections), associated with implanted or indwelling medical devices [101,102,104,105]. Venous and urinary catheters, orthopaedic prostheses, heart valves, pacemakers, cerebrospinal shunts, peritoneal dialysis devices represent the most typical and clinically relevant sites, where intractable and lethal biomaterial-associated infections (BAIs) can develop due to biofilm, thus worsening the patient's condition leading to the need of device removal[106,107]. In BAIs, the development of the infection depends on the type of implant and the length of time the implant is in the patient. The adhesion of pathogens to permanent medical devices is favoured by fibronectin and fibrinogen, which act as adhesion mediators for staphylococci[108].

Compound **1** Inhibits Biofilm Formation by The Strongest *Staphylococci* Biofilm Producers of Our Collection

On the worrying scenario depicted in the previous section, there is an urgent need to develop innovative anti-biofilm strategies specifically targeting the early adhesion and maturation processes of *S. aureus* and *S. epidermidis*, as current antimicrobial and anti-adhesive interventions frequently fail to effectively control these sessile communities. In this regard, compound **1** already discovered in this study as biocide against Gram-positive *S. aureus* at 4 × MIC (μg/mL), was here tested for assessing its possible capacity to inhibit biofilm formation by *Staphylococci*, at MIC, 2.5 × MIC and 5 × MICs (μg/mL), as described in the experimental section. Vancomycin was chosen as reference antibiotic, to which all selected clinical isolates were sensitive, which was administered at MIC, 2.5 × MIC and 5 × MICs (μg/mL), as compound **1**. The following Figure 6-8 show the biofilm formation inhibition (OD_{570}), the residual biofilm (%) and the biofilm inhibition (%) observed when 3 MRSA, 1 MSSA ATCC 29213 strain (sensitive to oxacillin) and 4 MRSE biofilm producers were not treated, or treated for 24 hours with **1** at MIC, 2.5 × MIC and 5 × MICs. Conversely, Figure S6.1-S6.2 in Section S6 in Supplementary Materials file show both the results obtained with vancomycin and **1** in single graphs for comparison and to have an idea of the potential of **1** in inhibiting the biofilm formation by the indicated strains

 doi:10.20944/preprints202603.0534.v1

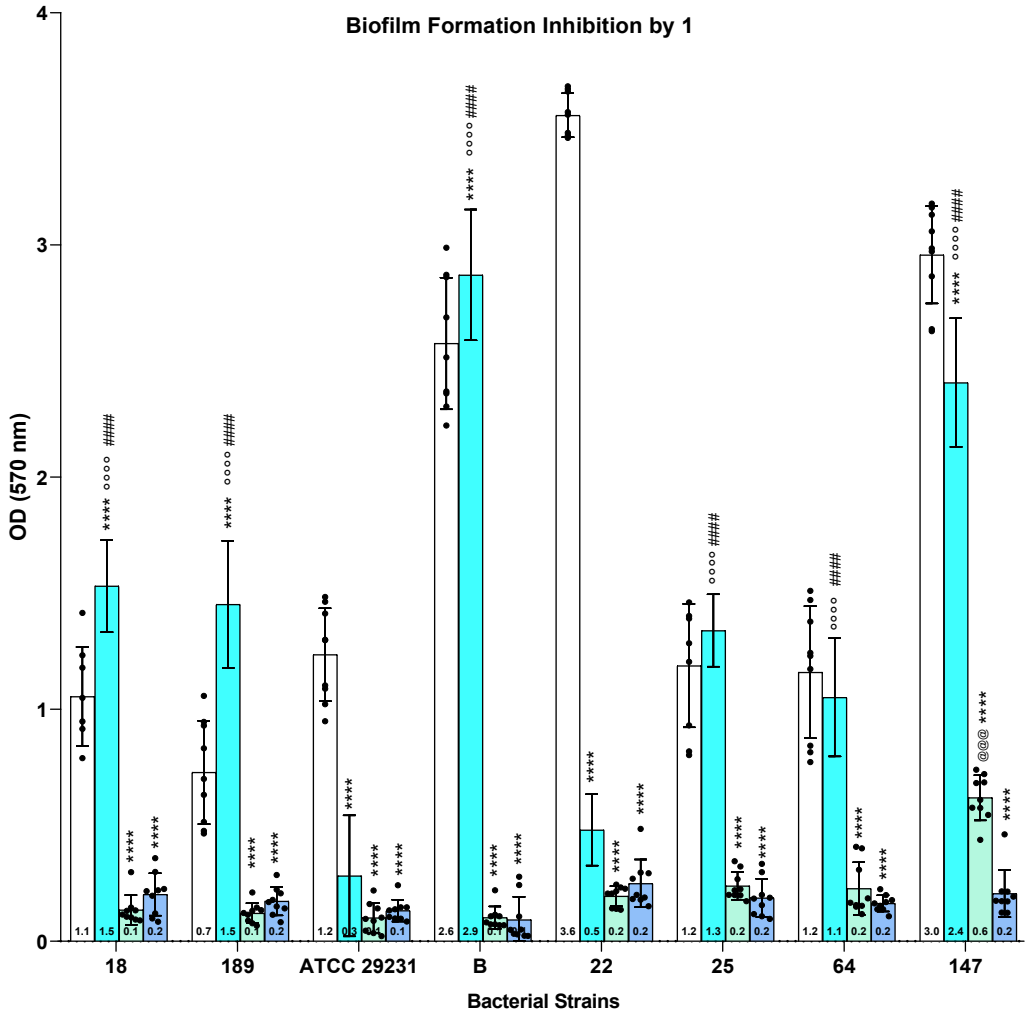

Figure 6. Inhibition of biofilm formation (OD 570 nm, OD_{570}) by four *S. aureus* (18, 189, ATCC 29213 and B) and four *S. epidermidis* (22, 25, 64 and 147) species induced by compound **1**, administered to bacteria at MIC (sky-blue bars), 2.5 × MIC (light-blue bars) and 5 × MIC (blue bars). Statistical significance was obtained using GraphPad PRISM software 8.0.1 by the analysis of variance (Two-ways ANOVA) corrected for multiple comparisons using statistical Tukey hypothesis testing. The statistical difference was reported for each isolate and for each concentration against control (CTR, white bars) using * symbol. Specifically, adjusted p values for multiplicity comparisons were reported for each comparison. Specifically, $p > 0.05$ no symbols; $p < 0.05$ *, $p < 0.01$ **, $p < 0.001$ *** and $p < 0.0001$ ****. Analogously, significant difference of MIC versus 2.5 and 5 × MIC was indicated using ° and # symbols, while statistical difference of 2.5 × MIC versus 5 × MIC was indicated using @ symbol.

 doi:10.20944/preprints202603.0534.v1

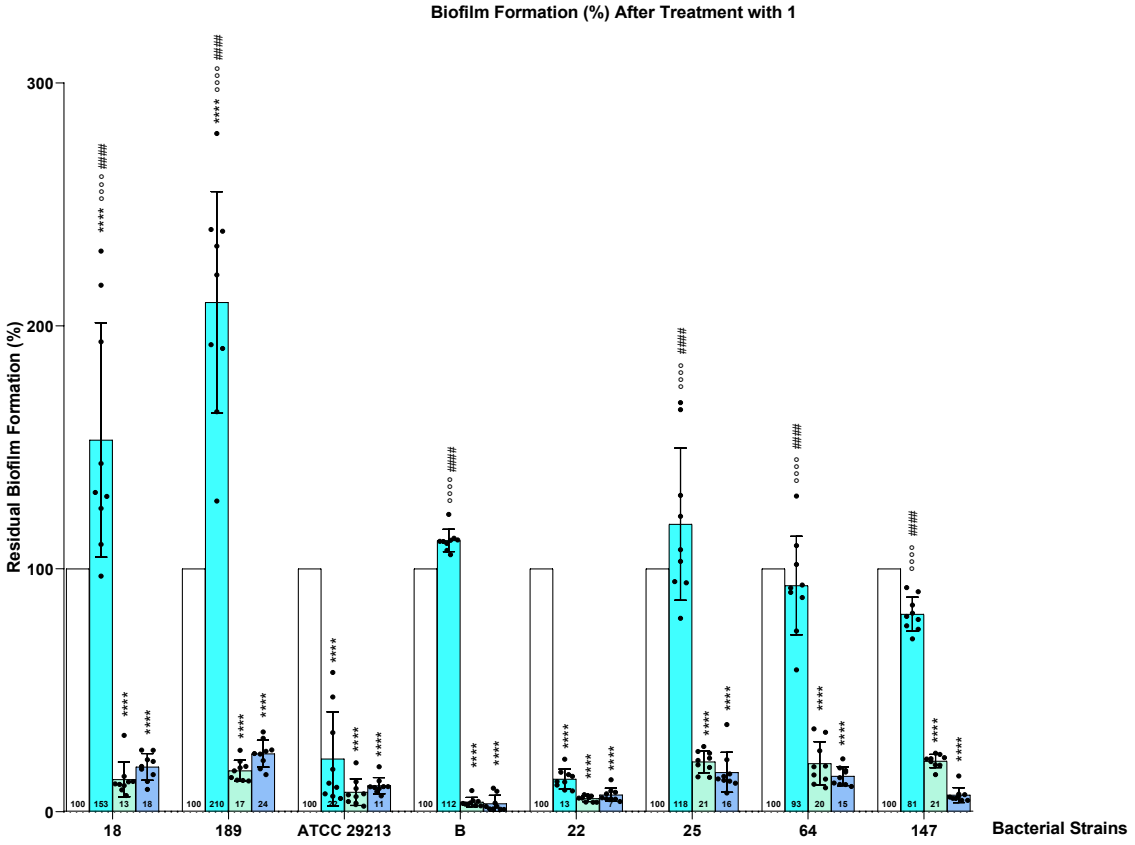

Figure 7. Residual biofilm formation (%) by *S. aureus* (18, 189, ATCC 29213 and B) and by *S. epidermidis* (22, 25, 64 and 147) species after treatments with compound **1** at MIC (sky-blue bars), 2.5 × MIC (light-blue bars) and 5 × MIC (blue bars). Statistical significance was obtained using GraphPad PRISM software 8.0.1 by the analysis of variance (Two-ways ANOVA) corrected for multiple comparisons using statistical Tukey hypothesis testing. The statistical difference was reported for each isolate and for each concentration against control fixed to 100% (CTR, white bars) using * symbol. Adjusted p values for multiplicity comparisons were reported for each comparison. Specifically, $p > 0.05$ no symbols; $p < 0.05$ *, $p < 0.01$ **, $p < 0.001$ *** and $p < 0.0001$ ****. Analogously, significant difference of MIC versus 2.5 and 5 × MIC was reported using ° and # symbols, while no statistical difference of 2.5 × MIC versus 5 × MIC was observed.

 doi:10.20944/preprints202603.0534.v1

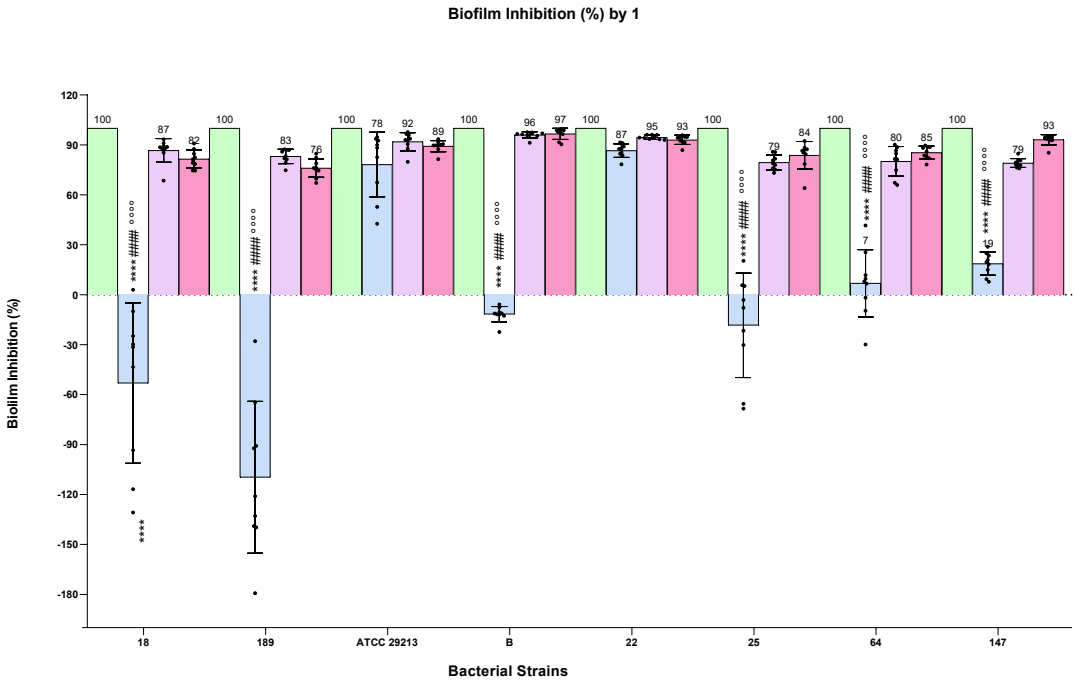

Figure 8. Biofilm inhibition percentage (%) after treatment of *S. aureus* (18, 189, ATCC 29213 and B) and *S. epidermidis* (22, 25, 64 and 147) species with compound **1**, administered to bacteria at MIC (light blue bars), 2.5 × MIC (violet bars) and 5 × MIC (pink bars). Statistical significance was obtained using GraphPad PRISM software 8.0.1 by the analysis of variance (Two-ways ANOVA), corrected for multiple comparisons using statistical Tukey hypothesis testing. The statistical difference was reported for each isolate and for each concentration tested against control (CTR, green bars) using * symbol. Adjusted *p* values for multiplicity comparisons were reported for each comparison. Specifically, $p > 0.05$ no symbols; $p < 0.05$ *, $p < 0.01$ **, $p < 0.001$ *** and $p < 0.0001$ ****. Significant difference of MIC versus 2.5 and 5 × MIC was reported using ° and # symbols. No statistical difference was observed for 2.5 versus 5 × MIC.

In the following presentation and discussion of results, *S. aureus* isolates were referred to, using SA and related isolate numbers, while *S. epidermidis* using SE. On this premise, despite the upper reliable detection limit for biofilm quantification by crystal violet staining (as made in this study) depends on the linearity range of the microplate reader instruments and typically ranges between OD 1.5 and 2.0, Stepanović (2007) and O'Toole (2011) et al [109,110], proposed the following classification (Table 7), according to which if an OD > 1.5–2.0 is observed, the isolate tested in a very strong biofilm producer.

Table 7. Classification of biofilm production based on OD [110].

OD (Optical Density)	Biofilm classification
< 0.1	Not adhering (No producer)
0.1 – 0.5	Weak biofilm producer
0.5 – 1.0	Moderate biofilm producer
> 1.0	Strong biofilm producer

Among *S. aureus* and *S. epidermidis* biofilm producers here considered all were very strong biofilm producers, except for *S. aureus* 18 and 189, which were moderate. *S. aureus* B (OD_{570} = 2.6), *S. epidermidis* 22 (OD_{570} = 3.6) and *S. aureus* B (OD_{570} = 2.9) were the major ones and especially *S. epidermidis* 22 (Figure 6). Despite this, when administered at 2.5 and 5 × MIC **1** was capable to

 doi:10.20944/preprints202603.0534.v1

remarkably ($p < 0.0001$) reduce biofilm formation by all strains (Figure 6), lowering OD_{570} values to 0.1-0.2, without any statistically significant differences among 2.5 and 5 × MIC, except in the case of *S. epidermidis* 147 (OD_{570} at 2.5 × MIC = 0.6, OD_{570} at 5 × MIC = 0.2). Collectively, biofilm production inhibition at these concentrations was of 76-95%, being in several cases major the inhibition caused by **1** administered at 2.5 × MIC, rather than that deriving by 5 × MIC. However, in three cases out of eight, the simple MIC administration of **1** was capable to significantly inhibit ($p < 0.0001$) biofilm formation by *S. aureus* ATCC 29213, as well as *S. epidermidis* 22 and 147, reducing their OD_{570} by 4, 7.2 and 1.25-fold, which mean a biofilm inhibition percentage (%) of 78, 87, and 19%. A lower inhibition of 7% was caused by **1** to the biofilm production by *S. epidermidis* 64. To date, antimicrobial peptides (AMPs) represent the most promising agents in counteract chronic infections caused by the biofilm produced by MDR superbugs[68]. New AMPs have been recently developed which demonstrated potent broad-spectrum sterilizing activity against a panel of Gram-positive and Gram-negative biofilms[68]. In this regard, Andreeva et al developed a library of several TPP-conjugate compounds and investigated the potential ability of lead compounds for the demonstrated MICs and MBCs (**4d**, **4e**, **4f**, **5d**, **5e**, and **5f**), both to inhibit the formation and to destroy the mature biofilm by not MRSA *S. aureus*, using crystal violet (CV) dye. Despite from the data showed by authors, which are only percentages not showing the OD values of untreated and treated bacteria, it is impossible to understand if biofilm producers they used are strong, mediocre or low, which should be a mandatory data, to weight correctly the observed inhibition, the most part of our results (%) concerning MRSA were like those by Andreeva et all. Specifically, except for compound **4c** which at MIC inhibited biofilm formation by almost 100%, four compounds by authors caused inhibition < 30% and compound **4f** inhibited the biofilm by about 85%[68]. Collectively, administration of 4-6 × MIC were necessary to all compounds by Andreeva to reach an inhibition in the range 80-100%. Here, **1** at MIC reduced *S. aureus* ATCC 29213 of 78%, while at 2.5-5 × MIC reduced biofilm formation by 83-97%. Additionally, **1** caused the 87, 7 and 19% reduction of biofilm produced *S. epidermidis* 22, 64 and 147, respectively at MIC. The same authors similarly reported the inhibition (%) of formation of biofilm by not MRSA *S. aureus* caused by two lead compounds (**4j** and **4m**) of another library of TPP-conjugates [69]. At concentrations of 2 × MIC (**4j**) and 4 × MIC (**4m**), the inhibition of *S. aureus* biofilm was more than 80%[69]. **1** caused the 87% biofilm inhibition (ATCC) at MIC and the 83-96% inhibition at 2.5 × MIC, thus outperforming both **4j** and **4m**. Both **1** and vancomycin, when administered at MIC concentration not inhibited biofilm by *S. epidermidis* 25 and 22, while vancomycin on the contrary of **1**, which failed in inhibiting their biofilm, inhibited biofilm formation by *S. aureus* 189 and AB, while **1** was better performant than vancomycin in inhibition the biofilm production by *S. aureus* ATCC 29213, as well as *S. epidermidis* 22, 64 and 147. Regardless their very different and not comparable specific MICs, a comparison between antibiofilm effects observed for **1** and reference antibiotic vancomycin, was anyway hazarded based on the same × MICs multiplication made for each of them (MIC, 2 and 5 × MICs). Both vancomycin and **1** remarkably inhibited biofilm formation by all bacteria tested at 2.5 and 5 × MIC. Specifically, at 2.5 × MIC vancomycin outperformed **1** in inhibiting biofilm by *S. aureus* 18 and 189, while the contrary was observed concerning the biofilm production by *S. aureus* ATCC 29213, B, *S. epidermidis* 22, 25, 64 and 147. Finally at 5 × MIC, **1** outperformed vancomycin concerning the inhibition of biofilm produced by *S. epidermidis* 22, 25, 64 and 147, while vancomycin was better than **1** in inhibiting biofilm formation by *S. aureus* 18, 189 and ATCC 29213. Collectively, the trend observed was that despite all bacteria were sensitive to vancomycin, this antibiotic functioned better than **1** against *S. aureus* while **1** against *S. epidermidis*. To investigate the intimate molecular mechanism supporting the capability of **1** to inhibit biofilm by *Staphylococci* used here was not in the scope of this already articulated study. Notably, such additional experiments would require a very expensive instruments and highly equipped core facilities and laboratories (BSL 2) [111–117]. Anyway, based on literature reports, it can be assumed that its antibiofilm capacity could depend on its high positive ζ-p of +38 [63]. Moreover, the use of vancomycin as reference antibiotic has evidenced that both vancomycin and **1** did function at sub-MICs values (not reported results) regardless their different MICs and need higher concentrations, in most cases over the MIC, to inhibit

 doi:10.20944/preprints202603.0534.v1

biofilm formation. Therefore, it could be rational to hypothesize for **1** in relation to its antibiofilm properties, a molecular mechanism like that of vancomycin. In this regard, it has been reported that, despite rather complex, the antibiofilm mechanism of vancomycin is based on few aspects. I was evidenced that vancomycin binds to peptidoglycan precursors, specifically to dipeptides D-ala-D-ala, in the reachable outer layers of young biofilm[118–120], thus preventing wall elongation[121,122]. Anyway, vancomycin, being a relatively large molecule, as **1**, has difficulty penetrating the biofilm's polysaccharide matrix, thus functioning only at high concentrations (as observed)[123,124] or when the biofilm is still young [120,125,126], thus weakening the overall structure, reducing bacterial adhesion to the substrate (catheters, implants) and making the bacteria more vulnerable to other agents, such as gentamicin [127]. Delivering of vancomycin by proper carriers can enhance its antibiofilm properties[128,129]. Several studies show that vancomycin is most effective before the biofilm is fully mature, by preventing bacterial division, impeding the production of the extracellular matrix and reducing the bacteria's ability to consolidate on the surface[125,130,131]. Assuming for **1** a similar behaviour, it can be also assumed that as for vancomycin, for already developed biofilms, combinations with other antibiotics or alternative strategies (enzymes, matrix-disrupting agents, etc.) will be necessary[132–134].

2.5. Cytotoxicity and Haemolytic Toxicity of Compound 1

2.5.1. Cytotoxicity of 1 Against Human Keratinocytes (HaCaT) and Murine Fibroblasts (3T3)

Cytotoxic effects of **1** against eukaryotic cells, such as HaCaT and 3T3 cells were essayed for 24, 48 and 72 hours, as reported in our recent article [18]. In that study, cells were administered with increasing concentrations of **1** in the range 1-100 μM and IC_{50} μM values were calculated by the WordPad software 8.0.1. (PRISM) using a non-linear fit model on opportunely transformed concentration data by an extrapolation, since viable cells were over 50% at all concentration tested. Only in the case of HaCaT cells exposed to **1** for 24 hours, a linear model was used since the software retained impossible extrapolate a reliable data using the non-linear one. Here results were converted in μg/mL and IC_{50} values after 24 hours exposure was considered and reported, to make possible a direct comparison with MICs determined after the same time as for EUCAST indications [52]. Figure 9A shows the results of cytotoxicity experiments carried out on HaCaT cells with compounds **1**, while Figure 9B those obtained on 3T3 cells.

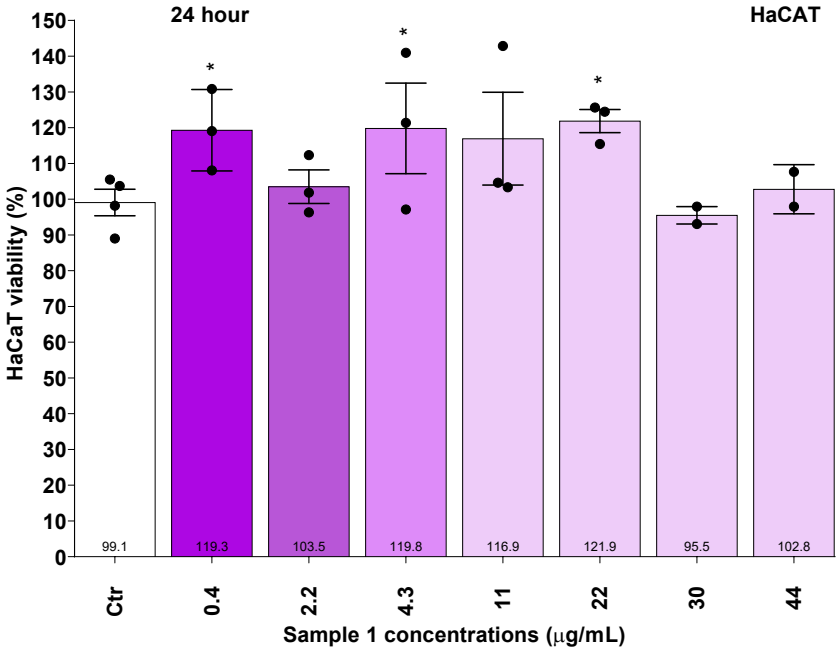

(A)

 doi:10.20944/preprints202603.0534.v1

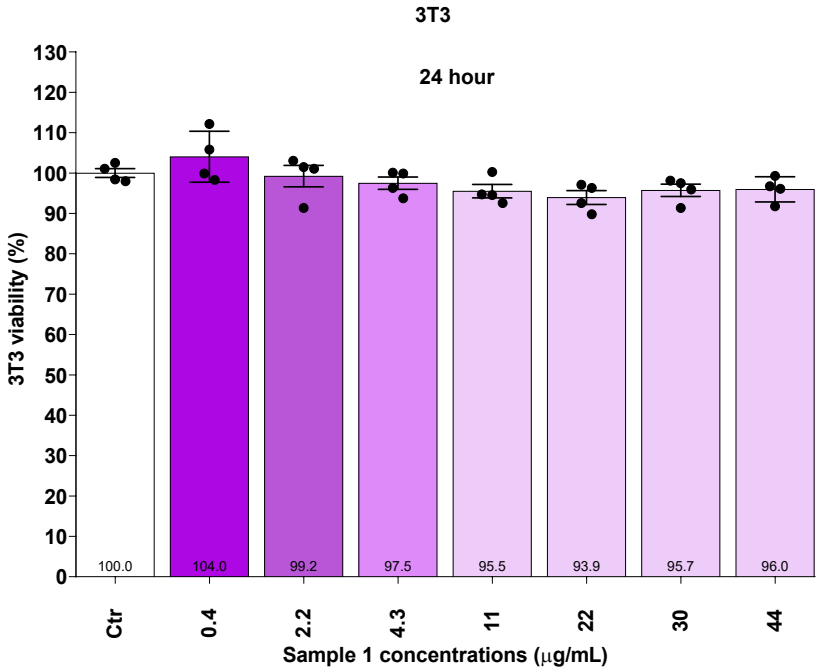

(B)

Figure 9. Cell viability was evaluated in HaCaT (A) and 3T3 (B) cells when exposed to increasing concentrations of **1** (0.4-44 µg/mL, 1–100 µM) for 24 hours. Bar graphs summarize quantitative data of the means ± S.D. of four independent experiments (black spheres) run in triplicate. Significance refers exclusively to control (*). Specifically, $p > 0.05$ no symbols; $p < 0.05$ * (one-way ANOVA followed by Dunnet's multi-comparisons test). Numbers at bottom within bars indicate viable cells (%).

As observable in Figure), viability of both cell populations was close to 100% and over, up to the high concentration tested (44µg/mL; 100 µM). Specifically, no significant difference in viability of 3T3 cells (%) versus control existed at all concentration tested, while the significant differences in viability of HaCaT cells (%) versus control detected at 0.4, 4.3 and 22 µg/mL regarded their proliferation.

2.5.2. Haemolytic Effects of 1 Against Red Blood Cells (RBCs)

As described for cytotoxic effects of **1** against eukaryotic cells, its haemolytic activity was investigated using RBCs according to a reported protocol [57] and detailed in our recent article[18]. In that study, RBCs were administered with increasing concentrations of **1** in the range 0.5-100 µM and the concentration of **1** necessary to kill the 50% of RCBs (HC_{50} µM values) were calculated by the WordPad software 8.0.1. (PRISM) using a non-linear fit model on opportunely transformed concentration data. Here results were converted in µg/mL to make possible a direct comparison with MICs. Figure 10 shows the RBCs viability (%), where concentrations 0.5-100 µM were expressed as µg/mL (0.2-43.3 µg/mL).

 doi:10.20944/preprints202603.0534.v1

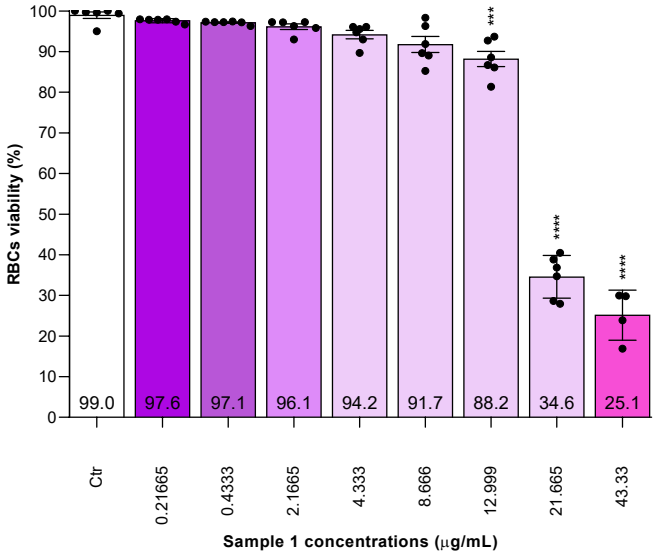

Figure 10. RBCs viability (%) as bars graph of untreated cells (Ctr, white bar) and after exposure to increasing concentrations of (0.2-43.3 µg/mL, 0.5-100.0 µM) of compound **1**. Experimental data are expressed as the mean ± S.D. of the data obtained on blood from six (black spheres) healthy donors. Significance is indicated exclusively vs. control (CTR) as follows: no symbols $p > 0.05$ and, *** $p < 0.001$ and **** $p < 0.0001$ (one-way ANOVA followed by Dunnet multi-comparisons test). Numbers at bottom within bars indicate viable cells (%).

Table 8 reports the HC_{50} values of **1** when tested on RBC for the time indicated by the protocol [57], and the IC_{50} ones when tested on HaCaT and 3T3 cells in 24 hours treatments as for bacteria to determine MICs.

Table 8. HC_{50} values of **1** when tested on RBC °, and IC_{50} when tested on HaCaT and 3T3 cells in 24 hours treatments as for bacteria to determine MICs.

Compound (MW)	Cells	IC_{50} (µg/mL)	HC_{50} (µg/mL)
1 (433.3)	RBCs	-	23.0±4.7
	HaCaT	216.7±V.W. *	-
	3T3	656.9± V.W. *	-

° Time of experiment according to protocol [57]. V.W. = very wide; * extrapolation; - not existent data.

2.5.3. Selectivity of 1 for Bacteria

Selectivity of **1** for bacteria in relation to its cytotoxicity against HaCaT and 3T3 cells and to its haemolytic toxicity against RBCs was investigated by calculating its selectivity index values (SIs). SIs are essentials to predict the therapeutic potential of a new compound which revealed certain antibacterial effects. Generally, the SIs against bacteria cells (BAs) in relation to eukaryotic cells (ECs) is calculated using the formula (1).

$$SI = MICs \text{ for } BCs / IC_{50} \text{ for } ECs \quad (1)$$

The HC_{50} and IC_{50} values reported in Table 8 were used to calculate the SIs of **1** against all Gram-positive clinical isolates used in this study according to Eq. 1. Results have been reported Table 9 and Figure 11.

 doi:10.20944/preprints202603.0534.v1

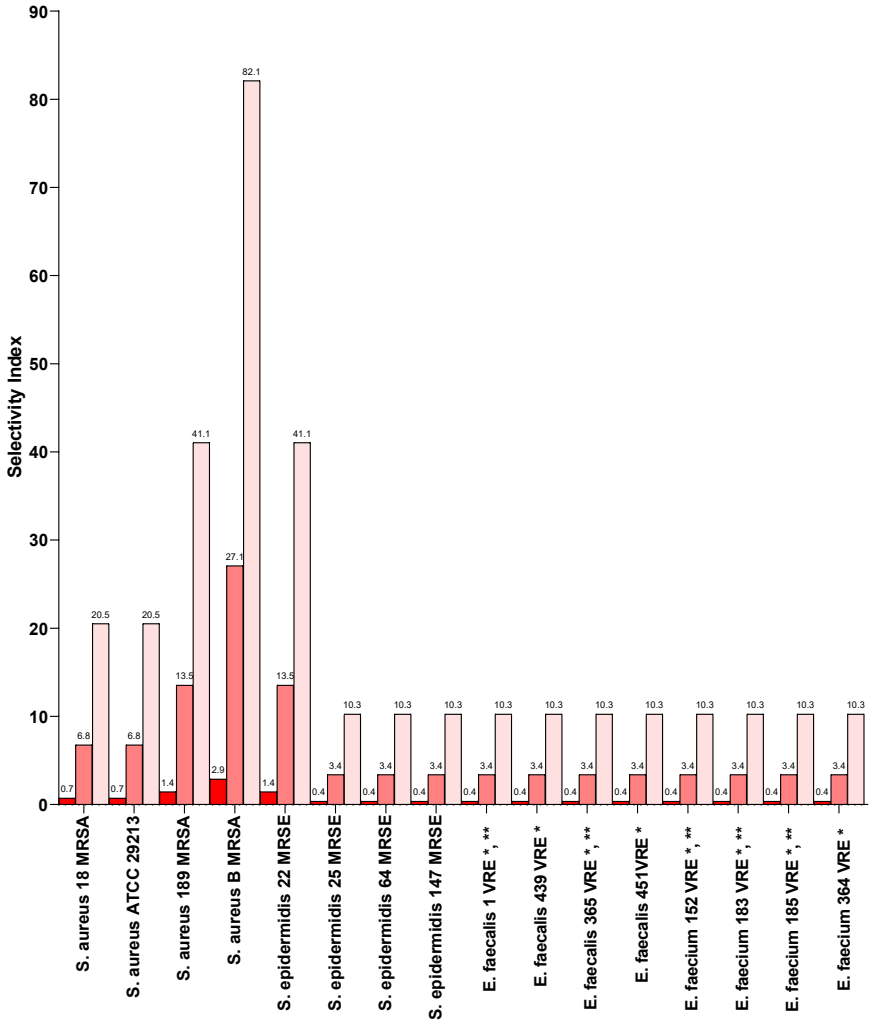

Figure 11. Selectivity index values (SIs) of **1** in relation to its haemolytic toxicity and cytotoxicity against RBCs (first red bars), as well as HaCaT (second strong-pink bars) and 3T3 cells (third soft-pink bars). VRE = vancomycin-resistant enterococci; MRSA = methicillin resistant *S. aureus*; MRSE = methicillin resistant *S. epidermidis*; * denotes resistance also to teicoplanin; ** denotes resistance also to linezolid. ATCC 29213 was a standard MSSA (sensitive to oxacillin).

Table 9. MICs of **1** against Gram-positive MDR clinical isolates used in this study and its selectivity index values (SIs) in relation to its haemolytic toxicity against RBCs and cytotoxicity against HaCaT and 3T3 cells.

Compounds	**1** (433.3) [1]	**SIs**		
Gram-positive Strains	**MIC (μg/mL)**	**RBCs**	**HaCaT**	**3T3**
S. aureus 18 MRSA	32	0.72	6.77	20.53
S. aureus ATCC 29213	32	0.72	6.77	20.53
S. aureus 189 MRSA	16	1.44	13.54	41.06
S. aureus B MRSA	8	2.88	27.09	82.11
S. epidermidis 22 MRSE	16	1.44	13.54	41.06
S. epidermidis 25 MRSE	64	0.36	3.39	10.26
S. epidermidis 64 MRSE	64	0.36	3.39	10.26
S. epidermidis 147 MRSE	64	0.36	3.39	10.26
E. faecalis 1 VRE *, **	64	0.36	3.39	10.26
E. faecalis 439 VRE *	64	0.36	3.39	10.26
E. faecalis 365 VRE *, **	64	0.36	3.39	10.26

 doi:10.20944/preprints202603.0534.v1

E. faecalis 451VRE *	64	0.36	3.39	10.26
E. faecium 152 VRE *, **	64	0.36	3.39	10.26
E. faecium 183 VRE *, **	64	0.36	3.39	10.26
E. faecium 185 VRE *, **	64	0.36	3.39	10.26
E. faecium 364 VRE *	64	0.36	3.39	10.26

[1] MW of compounds; VRE = vancomycin-resistant enterococci; MRSA = methicillin resistant *S. aureus*; MRSE = methicillin resistant *S. epidermidis*; * denotes resistance also to teicoplanin; ** denotes resistance also to linezolid.

According to data reported in Table and Figure 11 and SIs >1, **1** was safe for both HaCaT and 3T3 (SI = 3.4-27.1 and 10.3-82.1) cells, despite 3T3 were remarkably more tolerant to **1** than HaCaT cells in relation to its activity against all 16 strains tested in this study. Specifically, **1** was significantly safer and more indicate for treating infections by MRSA, rather than those by MRSE and VRE clinical isolates. Its safety to RBS resulted more critical. RBCs were significantly less tolerant to **1** than eukaryotic cell, establishing that it is advisable a clinical application of **1** via topic administration to treat infections sustained by all clinical isolates used in this study, especially for infections by MRSE and VRE. Anyway, if a rapid intervention is need and a systemic administration is necessary, it is advisable to use **1**, to treat infections by MRSA. Anyway, the haemolytic toxicity and cytotoxicity observed for **1** are lower than those observed for several TPP-contained QPSs already reported[33]. Recently, Nunes et al synthesised a series of quaternary heteronym salts including seven QPSs (**1a**-**1g**)[33]. They were microbiologically evaluated by the inhibition zone method and by determining their MICs and MBCs against ATCC bacteria. Bacteria included methicillin-resistant *S. aureus* ATCC 43300 (MRSA), *E. coli* ATCC 25922, *K. pneumoniae* K6/ESBL ATCC 700603, *P. aeruginosa* ATCC 27853, and *A. baumannii* ATCC 19606[33]. Their haemolytic toxicity (HC_{10}) versus RBCs (HC_{10} representing the concentrations causing 10% haemolysis) and cytotoxicity (IC_{50}) against human HEK293 cells (immortalized human epithelial embryonic hepatocytes, more used for transfection experiments than for vitality inhibition ones) were determined and selectivity index values, calculated [33]. Except for the less haemolytic compounds **1b** (SI > 128) and **1g** (SI > 128) in relation to their activity against ATCC 43300 MRSA, the haemolytic cytotoxicity of **1** vs. its activity against MRSA B and 189, were by 1.5-4.4-fold lower than that of all other compounds by Nunes and 1.22-2.20-times lower than that of compounds **1a**, **1d**, **1e** and **1f** [33]. On the other hand, only except for the less cytotoxic compound **1b** (SI > 128), all compounds by Nunes were more cytotoxic versus HEK293 in relation to their activity against ATCC MRSA, than **1** versus 3T3 cell in relation to its activity against all MRSA clinical isolates used here by 2.9-2625-times[33]. In a previous study, Nunes tested **1a**-1**g** against *S. aureus* CECT 976 sensitive to erythromycin, tetracycline, ciprofloxacin, ampicillin (MICs = 0.24-1.0 μg/mL) and oxacillin (MIC = 0.48 μg/mL), observing as lowest MIC value MICs = 2 μg/mL and as the highest one MICs > 64 μg/mL [32]. Intermediate MICs = 4, 8 and 32 μg/mL were also observed[32]. Subsequently the better performant compound **1e** was essayed against SA strains (*S. aureus* XU212, SA1199B, and RN4220), found by authors resistant to tetracycline (MIC = 128 μg/mL), to ciprofloxacin (MIC = 128 μg/mL) and to erythromycin (MIC = 256 μg/mL), respectively [32]. Anyway, only XU212 and SA1198B are reported as MRSA (MICs ≥ 4 μg/mL against oxacillin), since MICs reported for MSSE should be ≤ 2 μg/mL, and so like our MRSA, while RN4220 is a MSSA strain sensitive to oxacillin having MIC ≤ 2 μg/mL, and so like our ATCC 29213 standard strain[32]. MICs of **1e** were 1, 2 and 1 μg/mL while its IC_{50} against cancer hepatocytes HepG2 was about 5.4 μg/mL thus establishing SI values of 5.5, 2.25 and 5.5 in relation to its activity against XU212, SA1199B, and RN4220 strains respectively. Therefore, selectivity of **1** for MRSA and *S. aureus* ATCC 20213 in relation to its cytotoxicity to eukaryotic cells was higher than that of 1e for MRSA XU212, SA1199B and MSSA RN4220 by 1.2-29.8-times.

3. Materials and Methods

3.1. Compounds 1-4

 doi:10.20944/preprints202603.0534.v1

Compounds **1**, **3** and **4** (already found active against MDR resistant neuroblastoma and vemurafenib (PLX)-resistant melanoma cells [18] and therefore excellent applicants for having also antibacterial properties [19,24,26,27,29,31–34,42–50]), were in the form of quaternized phosphonium salts (QPSs). They encompassed the triphenyl benzyl (**1**) or the diphenyl-benzyl alkyl (**3** and **4**) phosphonium groups. The synthetic procedure to synthesize them and the phosphine compound **2**, never tested for potential biological effects, as well as methods followed to carry out their complete characterization, are detailed in a previous paper[18].

3.3. Optical Microscopy

The experimental details of optical microscopy analyses are reported in our recently published paper[18].

3.4. Dynamic Light Scattering Analysis (DLS)

The mean diameter (Z-average), polydispersity index (PDI), and zeta potential (ζ-p) of compounds **2**, **3** and **4**, as well as the ζ-p of **1**were measured at 25 °C using a Malvern Nano ZS90 light scattering apparatus (Malvern Instruments Ltd., Worcestershire, UK) at a scattering angle of 90° as previously described[51]. The apparent equivalent hydrodynamic radii of samples were calculated using the Stokes-Einstein equation. Since results showed more than one-dimensional family, analyses were acquired both by intensity and number (%), and results presented and discussed were those by number (%). Such type of acquisition permitted to ameliorate the peak of the most represented dimensional family, respect to that of other minor ones. Aliquots of compounds dispersions were withdrawn having count rate (kcps), sufficient for the analysis. The results from these experiments were expressed as mean ± SD of three measurements of ten runs per sample.

3.5. Microbiologic Experiments

3.5.1. Clinically Relevant Superbugs Used in This Study

A total of twenty-three strains belonging to a collection of MDR Gram-positive and Gram-negative species of the University of Genova, kindly gifted by S. Martino Hospital for research, were used in this study. All were isolated from human specimens for diagnosis purposes and identified using VITEKR 2 (Biomerieux, Firenze, Italy) or matrix-assisted laser desorption-ionization time-of-flight (MALDI-TOF) mass spectrometric technique (Biomerieux, Firenze, Italy). The isolates included sixteen Gram-positive and seven Gram-negative bacteria of different genera. Among bacteria of Gram-positive species, eight were enterococci (four *E. faecalis* and four *E. faecium*), while eight were staphylococci (four *S. aureus* and fours *S. epidermidis*). All enterococci were MDR isolates variously resistant to vancomycin or to teicoplanin (VRE), while all staphylococci, beside the *S. aureus* ATCC 29213 strain, were MDR strains with resistance to methicillin (MRSA and MRSE) and in some cases also to linezolid. Gram-negative species included five non-fermenting strains of *P. aeruginosa* isolated from cystic fibrosis patients with resistance to carbapenem and two strains of *Enterobacteriaceae*, consisting of one *E. coli* and one *K. pneumoniae* that were resistant to carbapenems by producing class A *K. pneumoniae* carbapenemase.

3.5.2. Determination of MICs

To investigate the antibacterial activity of compounds **1**-**4** on the described pathogens, their minimal inhibitory concentrations (MICs) were determined by following the microdilution procedure detailed by the European Committee on Antimicrobial Susceptibility Testing (EUCAST) [52] and reported in our previous works [26].

3.5.3. Time–Kill Curves

 doi:10.20944/preprints202603.0534.v1

Time–kill curve assays for compound **1** were performed on three representative isolates of *S. aureus* (strains 18 (MRSA), 189 (MRSA) and ATCC 29213 as previously reported [53–55]. A mid-logarithmic phase culture was diluted in Mueller–Hinton (MH) broth (Merck, Darmstadt, Germany) (10 mL) containing 4 × MIC of the selected compounds to give a final inoculum of 1.0×10^5 CFU/mL. The same inoculum was added to separate MH tubes as a growth control. Samples were incubated at 37 °C with constant shaking for 24 h. Aliquots of 0.20 mL from each tube were removed at 0, 1, 2, 4, 6, and 24 h, diluted appropriately with a 0.9% sodium chloride solution to avoid carryover of samples being tested, plated onto MH plates, and incubated for 24 h at 37 °C. Growth controls were run in parallel. The percentage of surviving bacterial cells was determined for each sampling time by comparing colony counts with those of standard dilutions of the growth control. Results have been expressed as $\log_{10}$ values of viable cell numbers (CFU/mL) of surviving bacterial cells over a 24 h period. A bactericidal effect was defined as a 3 $\log_{10}$ decrease of CFU/mL (99.9% killing) of the initial inoculum. All time–kill curve experiments were performed in triplicate.

3.5.4. Detection of Biofilm Production Using the Microliter Plate Method

Biofilm production was detected using the microliter plate method and quantified spectrophotometrically using a method based on that reported by Cramton et al.[56]. To produce biofilms, stationary-phase bacterial cultures of four *S. aureus* and *S. epidermidis* strains, known to be higher producers of biofilm (optical density at 570 nm, OD_{570} = 0.73-3.36) were diluted 1:100 aseptically to the wells of a 96-well polystyrene tissue culture plate (Corning, Milan, Italy) containing tryptic soy broth medium supplemented with 0.25% glucose and were incubated at 37 C for 24 h. To evaluate the effect of compound **1** and vancomycin, used as reference antibiotic, on biofilm synthesis, each compound was added to the growth medium at selected concentrations (MIC, 2.5 and 5 × MIC). After 24 h of exposure, media were discarded and each well was washed three times with phosphate-buffer saline to remove non-adherent cells. Plates were air-dried in an inverted position. Adherent microorganisms were stained with 0.1% crystal violet (CV). Excess stains were rinsed off with running tap water and the plates were air-dried. Adherent bacterial films were quantified spectrophotometrically by determining the OD_{570}. Each isolate was tested in triplicate. The results were derived from three separate experiments and OD_{570} values were expressed as mean ± standard deviation (S.D.). The OD_{570} value obtained for each strain without any added compound was used as the control (CTR). The percentages of residual biofilm formed in the presence of different concentrations of **1** and vancomycin were calculated employing the ratio between the values of OD_{570} with and without the compounds, adopting the following formula: [(OD_{570} with drug/OD_{570} without drug) × 100]. The biofilm percentage inhibition by two compounds were also calculated using the formula 100 - [(OD_{570} with drug/OD_{570} without drug) × 100].

Statistical Analysis

Statistical significance was obtained using GraphPad PRISM software 8.0.1 by the analysis of variance (Two-ways ANOVA) corrected for multiple comparisons using statistical Tukey hypothesis testing. The statistical difference of multiple comparisons was reported for each isolate, for each concentration and for each compound tested using symbols. Symbols used have been specified in this text and in Supplementary Materials (Section S6). Specifically, adjusted p values for multiplicity comparisons were reported for each comparison. No symbol was reported when $p > 0.5$. One symbol was used for $p < 0.1$, two, $p < 0.01$, three, $p < 0.001$ and four, $p < 0.0001$.

3.6. Cytotoxicity of Compound 1 on Eukaryotic Cells

Cytotoxic effects of **1** were essayed for 24 hours on human keratinocytes (HaCaT) and murine embryonic fibroblasts (3T3) as described in our recent paper[18].

3.7. Haemolytic Effects of Compound 1 on Red Blood Cells (RBCs)

 doi:10.20944/preprints202603.0534.v1

Haemolytic effects of **1** were essayed on red blood cells following the protocol [57] described in our recent papers [18,27,45,47].

4. Conclusions

With this study, we have revolutionized, updated and completed the microbiologic, haemolytic and cytotoxic behaviour of triphenyl benzyl phosphonium bromide, compound **1** in this study, previously essayed exclusively to assess its MICs. Compound **1** initially attracted our attention because a QPS compound, with already reported anticancer effects, and so probably endowed with antibacterial properties. Its double-faced activity was here confirmed, despite with results diametrically different for those reported by a single research group for it and very similar compounds. Unfortunately, double-checked results confirmed that **1** is fully inactive (for our standard of antibacterial activity) against Gram-negative species and especially against *P. aeruginosa*, while represent a new very promising bactericidal weapon to counteract Gram-positive MRSA, MRSE and VRE (*E. faecium* and *E. faecalis*). MICs in the range 8-64 μg/mL were determined for **1**, which was for the first time discovered to be bactericidal against MRSA clinical isolates and MSSA ATCC 29213 strains, within 11 hours from inoculum, without any regrowth in the subsequent hours up to 24. Additionally, for the first time **1** was essayed in antibiofilm experiments, which established its capability to inhibit biofilm formation by 3 MRSA, 1 MSSA ATCC 29213 strain, and 4 MRSE clinical isolates among the strongest biofilm producers of our collection (OD_{570} up to > 3), at MICs (7-87%), 2.5 (79-96%), and 5 × MICs (76-97%), depending on strains. According to data by recent experiments on RBCs, as well as on HaCaT and 3T3 cells, **1** was found to be less haemolytic and less cytotoxic versus eukaryotic cells, than the most part of very promising antibacterial QPSs recently reported. Collectively, these in vitro results pave the way for further experiments in vivo using proper animal models devoted to their confirmation.

Supplementary Materials: The following supporting information can be downloaded at the website of this paper posted on Preprints.org., Figure S1.1. ^{1}H NMR spectrum (400 MHz, $CHCl_3$) of compound 1. Figure S1.2. ^{13}C NMR spectrum (100 MHz, $CHCl_3$) of compound 1. Figure S1.3. ^{13}C NMR spectrum (600 MHz, $CHCl_3$) and DEPT135 experiment of compound 1. Figure S1.4. ^{31}P NMR spectrum (161 MHz, $CHCl_3$) of compound 1. Figure S1.5. ^{1}H NMR spectrum (400 MHz, $CHCl_3$) of compound 2. Figure S1.6. ^{13}C NMR spectrum (100 MHz, $CHCl_3$) of compound 2. Figure S1.7. ^{13}C NMR spectrum (600 MHz, $CHCl_3$) and DEPT135 experiment of compound 2. Figure S1.8. ^{31}P NMR spectrum (161 MHz, $CHCl_3$) of compound 2. Figure S1.9. ^{1}H NMR spectrum (400 MHz, $CHCl_3$) of compound 3. Figure S1.10. ^{13}C NMR spectrum (100 MHz, $CHCl_3$) of compound 3. Figure S1.11. ^{13}C NMR spectrum (600 MHz, $CHCl_3$) and DEPT135 experiment of compound 3. Figure S1.12. ^{31}P NMR spectrum (161 MHz, $CHCl_3$) of compound 3. Figure S1.13. ^{1}H NMR spectrum (400 MHz, $CHCl_3$) of compound 4. Figure S1.14. ^{13}C NMR spectrum (100 MHz, $CHCl_3$) of compound 4. Figure S1.15. ^{13}C NMR spectrum (600 MHz, $CHCl_3$) and DEPT135 experiment of compound 4. Figure S1.16. ^{31}P NMR spectrum (161 MHz, $CHCl_3$) of compound 4. Figure S2.1. ATR-FTIR spectrum of 1. Figure S2.2. ATR-FTIR spectrum of 2. Figure S2.3. ATR-FTIR spectrum of 3. Figure S2.4. ATR-FTIR spectrum of 4. Figure S3.1. UV-Vis spectra of compounds 1-4 achieved reporting in graph the standardized csv data provided by the spectrometer using Microsoft 365 Excel software (a) and the not standardized one with peak labels added (b). Figure 4.1. Vesicular aggregates of 2 (A, B, C, D), 3 (E, F, G, H) and 4 (I, J, K,L), as well as crystals of 1 (M, N, O, P) in MeOH (A, C, E, G, I, K, M, O) and in water solution (B, D, F, H, J, L, N,P) observed with a 40× objective (A, B, E, F, I, J, M, N,). Smaller spherical vesicles of same compound were better evidenced using the 100× objective (C, D, G, H, K, L, O, P). Figure S5.1. Three acquisitions of the DLS analyses on compound 4 by intensity (%) (water, kcps = 20.2-20.5). Explanation of the image content is in the main text. Figure S5.2. Three acquisitions of the DLS analyses on compound 2 by number (%) (water, kcps = 7.2-14.2). Explanation of the image content is in the main text. Figure S5.3. Two acquisitions of the DLS analyses on compound 3 by number (%), (water, kcps = 11.3-14.2). Explanation of the image content is in the main text. Figure S6.1. Residual biofilm formation after treatment of *Staphylococcus aureus* (18, 189, ATCC 29213 and B), *S. epidermidis* (22, 25, 64 and 147) species sensitive to vancomycin, with compound 1 (lighter colours and dispar numbers bars) and vancomycin used as reference antibiotic (darker colours and pair numbers bars) administered

 doi:10.20944/preprints202603.0534.v1

to bacteria at MIC (blue bars), 2.5 × MIC (violet bars) and 5 × MIC (pink-red bars) for the specific drug. Statistical significance was obtained using GraphPad PRISM software 8.0.1 by the analysis of variance (Two-ways ANOVA) corrected for multiple comparisons using statistical Tukey hypothesis testing. The statistical difference was reported for each isolate and for each concentration tested against control (CTR, green bars) using * symbol only for vancomycin (not reported previously). Adjusted p values for multiplicity comparisons were reported for each comparison. Specifically, $p > 0.05$ no symbols; $p < 0.05$ *, $p < 0.01$ **, $p < 0.001$ *** and $p < 0.0001$ ****. Analogously, statistical differences of controls of 1 and those of vancomycin were reported using $ symbols. Then significant difference of MIC of vancomycin versus its 2.5 and 5 × MIC was reported using # and § symbols, while statistical difference of 2.5 × MIC of vancomycin versus its 5 × MIC was reports using & symbol. Additionally, significant difference of MIC of vancomycin versus 2.5 and 5 × MIC of 1 was indicated using c and d symbols, while that of MIC of 1 versus MIC, 2.5 and 5 × MIC of vancomycin was indicated with °, a and b symbols. Significant differences of 2.5 × MIC of 1 versus 2.5 and 5 × MIC of vancomycin were indicated with 0 and % symbols, while that of 5 × MIC of 1 versus 5 × MIC vancomycin with £ symbol. Figure S6.2. Biofilm inhibition percentage (%) after treatment of *Staphylococcus aureus* (18, 189, ATCC 29213 and B), *S. epidermidis* (22, 25, 64 and 147) species sensitive to vancomycin, with compound 1 (lighter colours and dispar numbers bars) and vancomycin used as reference antibiotic (darker colours and pair numbers bars) administered to bacteria at MIC (blue bars), 2.5 × MIC (violet bars) and 5 × MIC (pink-red bars) for the specific drug. Statistical significance was obtained using GraphPad PRISM software 8.0.1 by the analysis of variance (Two-ways ANOVA) corrected for multiple comparisons using statistical Tukey hypothesis testing. The statistical difference was reported for each isolate and for each concentration tested against control (CTR, green bars) using * symbol only for vancomycin (not reported previously). Adjusted p values for multiplicity comparisons were reported for each comparison. Specifically, $p > 0.05$ no symbols; $p < 0.05$ *, $p < 0.01$ **, $p < 0.001$ *** and $p < 0.0001$ ****. Analogously, statistical differences of controls of 1 and those of vancomycin was reported using $ symbols. Then significant difference of MIC of vancomycin versus its 2.5 and 5 × MIC was reported using # and § symbols, while statistical difference of 2.5 × MIC of vancomycin versus its 5 × MIC was reported using & symbol. Additionally, significant difference of MIC vancomycin versus 2.5 and 5 × MIC of 1 was indicated using c and d symbols, while that of MIC of 1 versus MIC, 2.5 and 5 × MIC of vancomycin was indicated with °, a and b symbols. Significant differences of 2.5 × MIC of 1 versus 2.5 and 5 × MIC of vancomycin were indicated with 0 and % symbols, while that of 5 × MIC of 1 versus 5 × MIC vancomycin with £ symbol.

Author Contributions: Conceptualization, methodology, software, validation, formal analysis, investigation, resources, S.A and A.M.S. Writing—original draft preparation, data curation, S.A. Writing—review and editing, project administration, S.A. and A.M.S. G.P. cured the identification of bacterial species and their pattern of resistance; DLS analyses acquisition, G.Z. and C.R. All authors have read and agreed to the published version of the manuscript.

Funding: This research was not supported by funds.

Data Availability Statement: All research data related to this study are available in the main text and in the Supplementary Materials file associated to this article available at https://www.mdpi.com/article/doi/s1.

Acknowledgments: Authors are very grateful to Paolo Giordani for the acquisition of optical images and to Paolo Oliveri for the acquisition of ATR-FTIR and UV-Vis spectra, reported in Supplementary Materials.

Conflicts of Interest: The authors declare no conflicts of interest.

References

1. Chandrasekhar, D.; Joseph, C.M.; parambil, J.C.; Murali, S.; Yahiya, M.; K, S. Superbugs: An Invicible Threat in Post Antibiotic Era. *Clin. Epidemiol. Glob. Health* **2024**, *28*, doi:10.1016/j.cegh.2023.101499.
2. Rajendran, R. Superbug Infection. *J. Drug Metab. Toxicol.* **2018**, *09*, doi:10.4172/2157-7609.1000238.
3. Mancuso, G.; Midiri, A.; Gerace, E.; Biondo, C. Bacterial Antibiotic Resistance: The Most Critical Pathogens. *Pathogens* 2021, *10*.

 doi:10.20944/preprints202603.0534.v1

4. Murray, C.J.L.; Ikuta, K.S.; Sharara, F.; Swetschinski, L.; Robles Aguilar, G.; Gray, A.; Han, C.; Bisignano, C.; Rao, P.; Wool, E.; et al. Global Burden of Bacterial Antimicrobial Resistance in 2019: A Systematic Analysis. *The Lancet* **2022**, *399*, 629–655, doi:10.1016/S0140-6736(21)02724-0.
5. Lakhundi, S.; Zhang, K. Methicillin-Resistant Staphylococcus Aureus: Molecular Characterization, Evolution, and Epidemiology. *Clin. Microbiol. Rev.* **2018**, *31*, doi:10.1128/CMR.00020-18.
6. Liu, Y.; Lu, H.; Hu, G.; Liu, J.; Lian, S.; Pang, S.; Zhu, G.; Ding, X. Unmasking MRSA's Armor: Molecular Mechanisms of Resistance and Pioneering Therapeutic Countermeasures. *Microorganisms* **2025**, *13*, 1928, doi:10.3390/microorganisms13081928.
7. Le, K.Y.; Otto, M. Approaches to Combating Methicillin-Resistant *Staphylococcus Aureus* (MRSA) Biofilm Infections. *Expert Opin. Investig. Drugs* **2024**, *33*, 1–3, doi:10.1080/13543784.2024.2305136.
8. Lebeaux, D.; Ghigo, J.-M.; Beloin, C. Biofilm-Related Infections: Bridging the Gap between Clinical Management and Fundamental Aspects of Recalcitrance toward Antibiotics. *Microbiology and Molecular Biology Reviews* **2014**, *78*, 510–543, doi:10.1128/MMBR.00013-14.
9. Otto, M. Staphylococcus Epidermidis — the "accidental" Pathogen. *Nat. Rev. Microbiol.* **2009**, *7*, 555–567, doi:10.1038/nrmicro2182.
10. Becker, K.; Heilmann, C.; Peters, G. Coagulase-Negative Staphylococci. *Clin. Microbiol. Rev.* **2014**, *27*, 870–926, doi:10.1128/CMR.00109-13.
11. McCann, M.T.; Gilmore, B.F.; Gorman, S.P. *Staphylococcus Epidermidis* Device-Related Infections: Pathogenesis and Clinical Management. *Journal of Pharmacy and Pharmacology* **2008**, *60*, 1551–1571, doi:10.1211/jpp.60.12.0001.
12. Trobos, M.; Firdaus, R.; Svensson Malchau, K.; Tillander, J.; Arnellos, D.; Rolfson, O.; Thomsen, P.; Lasa, I. Genomics of Staphylococcus Aureus and Staphylococcus Epidermidis from Periprosthetic Joint Infections and Correlation to Clinical Outcome. *Microbiol. Spectr.* **2022**, *10*, doi:10.1128/spectrum.02181-21.
13. Takahashi, C.; Sato, M.; Sato, C. Biofilm Formation of Staphylococcus Epidermidis Imaged Using Atmospheric Scanning Electron Microscopy. *Anal. Bioanal. Chem.* **2021**, *413*, 7549–7558, doi:10.1007/s00216-021-03720-x.
14. Arias, C.A.; Contreras, G.A.; Murray, B.E. Management of Multidrug-Resistant Enterococcal Infections. *Clinical Microbiology and Infection* **2010**, *16*, 555–562, doi:10.1111/j.1469-0691.2010.03214.x.
15. Arias, C.A.; Murray, B.E. The Rise of the Enterococcus: Beyond Vancomycin Resistance. *Nat. Rev. Microbiol.* **2012**, *10*, 266–278, doi:10.1038/nrmicro2761.
16. Lee, T.; Pang, S.; Abraham, S.; Coombs, G.W. Antimicrobial-Resistant CC17 Enterococcus Faecium: The Past, the Present and the Future. *J. Glob. Antimicrob. Resist.* **2019**, *16*, 36–47, doi:10.1016/j.jgar.2018.08.016.
17. Mohamed, J.A.; Huang, D.B. Biofilm Formation by Enterococci. *J. Med. Microbiol.* **2007**, *56*, 1581–1588, doi:10.1099/jmm.0.47331-0.
18. Alfei, S.; Signorello, M.G.; Tinedi, S.; Khaledizadeh, E.; Giordani, P.; Reggio, C.; Marengo, B.; Domenicotti, C. Quaternary Phosphonium Salts Outperformed Vemurafenib (PLX) and Etoposide Against BRAF^{V600D, V600E} PLX-Resistant, Melanoma and MDR Neuroblastoma, Exhibiting No/Low Toxicity on 3T3/HaCaT Cells 2026.
19. Kodjo Amengor, C.D.; Amaning Danquah, C.; Adusei, E.B.A.; Kekessie, F.K.; Ofosu-Koranteng, F.; Peprah, P.; Harley, B.K.; Orman, E.; Adu, J.; Saaka, Y. Synthesized Phosphonium Compounds Demonstrate Resistant Modulatory and Antibiofilm Formation Activities against Some Pathogenic Bacteria. *Heteroatom Chemistry* **2022**, *2022*, 1–9, doi:10.1155/2022/7411957.
20. Parchebafi, A.; Tamanaee, F.; Ehteram, H.; Ahmad, E.; Nikzad, H.; Haddad Kashani, H. The Dual Interaction of Antimicrobial Peptides on Bacteria and Cancer Cells; Mechanism of Action and Therapeutic Strategies of Nanostructures. *Microb. Cell Fact.* **2022**, *21*, 118, doi:10.1186/s12934-022-01848-8.
21. Zając, M.; Kotyńska, J.; Zambrowski, G.; Breczko, J.; Deptuła, P.; Cieśluk, M.; Zambrzycka, M.; Święcicka, I.; Bucki, R.; Naumowicz, M. Exposure to Polystyrene Nanoparticles Leads to Changes in the Zeta Potential of Bacterial Cells. *Sci. Rep.* **2023**, *13*, 9552, doi:10.1038/s41598-023-36603-5.
22. Vejzovic, D.; Piller, P.; Cordfunke, R.A.; Drijfhout, J.W.; Eisenberg, T.; Lohner, K.; Malanovic, N. Where Electrostatics Matter: Bacterial Surface Neutralization and Membrane Disruption by Antimicrobial Peptides SAAP-148 and OP-145. *Biomolecules* **2022**, *12*, 1252, doi:10.3390/biom12091252.

 doi:10.20944/preprints202603.0534.v1

23. Halder, S.; Yadav, K.K.; Sarkar, R.; Mukherjee, S.; Saha, P.; Haldar, S.; Karmakar, S.; Sen, T. Alteration of Zeta Potential and Membrane Permeability in Bacteria: A Study with Cationic Agents. *Springerplus* **2015**, *4*, 672, doi:10.1186/s40064-015-1476-7.
24. Khan, F.; Saha, P.; Bera, D.; Das, S. Structure Activity Relationship of Novel Antibacterial Phosphonium Ionic Liquids/Organic Salts in Dispersions and on Films: Potential Antifouling Coating Materials. *Mater. Chem. Phys.* **2023**, *309*, 128389, doi:10.1016/J.MATCHEMPHYS.2023.128389.
25. Alfei, S.; Schito, A.M. Positively Charged Polymers as Promising Devices against Multidrug Resistant Gram-Negative Bacteria: A Review. *Polymers (Basel).* **2020**, *12*, 1195, doi:10.3390/polym12051195.
26. Bacchetti, F.; Schito, A.M.; Milanese, M.; Castellaro, S.; Alfei, S. Anti Gram-Positive Bacteria Activity of Synthetic Quaternary Ammonium Lipid and Its Precursor Phosphonium Salt. *Int. J. Mol. Sci.* **2024**, *25*, 2761, doi:10.3390/ijms25052761.
27. Alfei, S.; Zuccari, G.; Bacchetti, F.; Torazza, C.; Milanese, M.; Siciliano, C.; Athanassopoulos, C.M.; Piatti, G.; Schito, A.M. Synthesized Bis-Triphenyl Phosphonium-Based Nano Vesicles Have Potent and Selective Antibacterial Effects on Several Clinically Relevant Superbugs. *Nanomaterials* **2024**, *14*, 1351, doi:10.3390/nano14161351.
28. Graikioti, D.; Athanassopoulos, C.M.; Schito, A.M.; Alfei, S. Synthesis and Characterization of Triphenyl Phosphonium-Modified Triterpenoids with Never Reported Antibacterial Effects Against Clinically Relevant Gram-Positive Superbugs 2025.
29. Ermolaev, V.; Miluykov, V.; Rizvanov, I.; Krivolapov, D.; Zvereva, E.; Katsyuba, S.; Sinyashin, O.; Schmutzler, R. Phosphonium Ionic Liquids Based on Bulky Phosphines: Synthesis, Structure and Properties. *Dalton Transactions* **2010**, *39*, 5564, doi:10.1039/b924636c.
30. Arkhipova, D.M.; Samigullina, A.I.; Minyaev, M.E.; Lyubina, A.P.; Voloshina, A.D.; Ermolaev, V. V. Synthesis, Crystal Structure, and Biological Activity of Menthol-Based Chiral Quaternary Phosphonium Salts (CQPSs). *Struct. Chem.* **2024**, *35*, 75–88, doi:10.1007/s11224-023-02259-0.
31. Ermolaev, V. V.; Arkhipova, D.M.; Miluykov, V.A.; Lyubina, A.P.; Amerhanova, S.K.; Kulik, N. V.; Voloshina, A.D.; Ananikov, V.P. Sterically Hindered Quaternary Phosphonium Salts (QPSs): Antimicrobial Activity and Hemolytic and Cytotoxic Properties. *Int. J. Mol. Sci.* **2021**, *23*, 86, doi:10.3390/ijms23010086.
32. Nunes, B.; Cagide, F.; Fernandes, C.; Borges, A.; Borges, F.; Simões, M. Efficacy of Novel Quaternary Ammonium and Phosphonium Salts Differing in Cation Type and Alkyl Chain Length against Antibiotic-Resistant Staphylococcus Aureus. *Int. J. Mol. Sci.* **2023**, *25*, 504, doi:10.3390/ijms25010504.
33. Nunes, B.; Cagide, F.; Borges, F.; Simões, M. Antimicrobial Activity and Cytotoxicity of Novel Quaternary Ammonium and Phosphonium Salts. *J. Mol. Liq.* **2024**, *401*, 124616, doi:10.1016/j.molliq.2024.124616.
34. Banerjee, A.; Aremu, B.R.; Dehghandokht, S.; Salama, R.; Zhou, H.; Lackie, S.M.; Seifi, M.; Kennepohl, P.; Trant, J.F. Lethal Weapon IL: A Nano-Copper/Tetraalkylphosphonium Ionic Liquid Composite Material with Potent Antibacterial Activity. *RSC Sustainability* **2023**, *1*, 1783–1797, doi:10.1039/D3SU00203A.
35. Mukherjee, I.; Manna, K.; Dinda, G.; Ghosh, S.; Moulik, S.P. Shear- and Temperature-Dependent Viscosity Behavior of Two Phosphonium-Based Ionic Liquids and Surfactant Triton X-100 and Their Biocidal Activities. *J. Chem. Eng. Data* **2012**, *57*, 1376–1386, doi:10.1021/je200938k.
36. Das, S.; Paul, A.; Bera, D.; Dey, A.; Roy, A.; Dutta, A.; Ganguly, D. Design, Development and Mechanistic Insights into the Enhanced Antibacterial Activity of Mono and Bis-Phosphonium Fluoresceinate Ionic Liquids. *Mater. Today Commun.* **2021**, *28*, 102672, doi:10.1016/j.mtcomm.2021.102672.
37. Metelytsia, L.O.; Hodyna, D.M.; Semenyuta, I. V.; Kovalishyn, V. V.; Rogalsky, S.P.; Derevianko, K.Y.; Brovarets, V.S.; Tetko, I. V. Theoretical and Experimental Studies of Phosphonium Ionic Liquids as Potential Antibacterials of MDR Acinetobacter Baumannii. *Antibiotics* **2022**, *11*, 491, doi:10.3390/antibiotics11040491.
38. O'Toole, G.A.; Wathier, M.; Zegans, M.E.; Shanks, R.M.Q.; Kowalski, R.; Grinstaff, M.W. Diphosphonium Ionic Liquids as Broad-Spectrum Antimicrobial Agents. *Cornea* **2012**, *31*, 810–816, doi:10.1097/ICO.0b013e31823f0a86.
39. Terekhova, N. V.; Khailova, L.S.; Rokitskaya, T.I.; Nazarov, P.A.; Islamov, D.R.; Usachev, K.S.; Tatarinov, D.A.; Mironov, V.F.; Kotova, E.A.; Antonenko, Y.N. Trialkyl(Vinyl)Phosphonium Chlorophenol

 doi:10.20944/preprints202603.0534.v1

Derivatives as Potent Mitochondrial Uncouplers and Antibacterial Agents. *ACS Omega* **2021**, *6*, 20676–20685, doi:10.1021/acsomega.1c02909.

40. Simões, M.; Pereira, A.R.; Simões, L.C.; Cagide, F.; Borges, F. Biofilm Control by Ionic Liquids. *Drug Discov. Today* **2021**, *26*, 1340–1346, doi:10.1016/J.DRUDIS.2021.01.031.
41. Pendleton, J.N.; Gilmore, B.F. The Antimicrobial Potential of Ionic Liquids: A Source of Chemical Diversity for Infection and Biofilm Control. *Int. J. Antimicrob. Agents* **2015**, *46*, 131–139, doi:10.1016/J.IJANTIMICAG.2015.02.016.
42. Galkina, I.; Bakhtiyarova, Y.; Andriyashin, V.; Galkin, V.; Cherkasov, R. Synthesis and Antimicrobial Activities of Phosphonium Salts on Basis of Triphenylphosphine and 3,5-Di-Tert-Butyl-4-Hydroxybenzyl Bromide. *Phosphorus Sulfur Silicon Relat. Elem.* **2013**, *188*, 15–18, doi:10.1080/10426507.2012.740694.
43. Terekhova, N. V.; Tatarinov, D.A.; Shaihutdinova, Z.M.; Pashirova, T.N.; Lyubina, A.P.; Voloshina, A.D.; Sapunova, A.S.; Zakharova, L.Ya.; Mironov, V.F. Design and Synthesis of Amphiphilic 2-Hydroxybenzylphosphonium Salts with Antimicrobial and Antitumor Dual Action. *Bioorg. Med. Chem. Lett.* **2020**, *30*, 127234, doi:10.1016/j.bmcl.2020.127234.
44. Alfei, S.; Zuccari, G.; Athanassopoulos, C.M.; Domenicotti, C.; Marengo, B. Strongly ROS-Correlated, Time-Dependent, and Selective Antiproliferative Effects of Synthesized Nano Vesicles on BRAF Mutant Melanoma Cells and Their Hyaluronic Acid-Based Hydrogel Formulation. *Int. J. Mol. Sci.* **2024**, *25*, 10071, doi:10.3390/ijms251810071.
45. Alfei, S.; Torazza, C.; Bacchetti, F.; Signorello, M.G.; Passalacqua, M.; Domenicotti, C.; Marengo, B. Tri-Phenyl-Phosphonium-Based Nano Vesicles: A New In Vitro Nanomolar-Active Weapon to Eradicate PLX-Resistant Melanoma Cells. *Int. J. Mol. Sci.* **2025**, *26*, 3227, doi:10.3390/ijms26073227.
46. Alfei, S.; Giannoni, P.; Signorello, M.G.; Torazza, C.; Zuccari, G.; Athanassopoulos, C.M.; Domenicotti, C.; Marengo, B. The Remarkable and Selective In Vitro Cytotoxicity of Synthesized Bola-Amphiphilic Nanovesicles on Etoposide-Sensitive and -Resistant Neuroblastoma Cells. *Nanomaterials* **2024**, *14*, 1505, doi:10.3390/nano14181505.
47. Alfei, S.; Torazza, C.; Bacchetti, F.; Milanese, M.; Passalaqua, M.; Khaledizadeh, E.; Vernazza, S.; Domenicotti, C.; Marengo, B. TPP-Based Nanovesicles Kill MDR Neuroblastoma Cells and Induce Moderate ROS Increase, While Exert Low Toxicity To-Wards Primary Cell Cultures: An in Vitro Study . *IJMS* **2025**, *26*, 4991, doi:https://doi.org/10.3390/ijms26114991.
48. Cieniecka-Rosłonkiewicz, A.; Pernak, J.; Kubis-Feder, J.; Ramani, A.; Robertson, A.J.; Seddon, K.R. Synthesis, Anti-Microbial Activities and Anti-Electrostatic Properties of Phosphonium-Based Ionic Liquids. *Green Chemistry* **2005**, *7*, 855, doi:10.1039/b508499g.
49. Milenković, M.R.; Živković-Radovanović, V.; Andjelković, L. Synthesis and Antimicrobial Activity of (3-Formyl-4-Hydroxybenzyl)Triphenylphosphonium Chloride Acylhydrazones. *Russ. J. Gen. Chem.* **2020**, *90*, 1716–1720, doi:10.1134/S1070363220090194.
50. Valenti, G.E.; Alfei, S.; Caviglia, D.; Domenicotti, C.; Marengo, B. Antimicrobial Peptides and Cationic Nanoparticles: A Broad-Spectrum Weapon to Fight Multi-Drug Resistance Not Only in Bacteria. *Int. J. Mol. Sci.* **2022**, *23*, 6108, doi:10.3390/ijms23116108.
51. Zuccari, G.; Zorzoli, A.; Marimpietri, D.; Alfei, S. Development of Mixed Micelles for Enhancing Fenretinide Apparent Solubility and Anticancer Activity Against Neuroblastoma Cells. *Curr. Drug Deliv.* **2025**, *22*, 1017–1029, doi:10.2174/0115672018333862240830072536.
52. EUCAST. European Committee on Antimicrobial Susceptibility Testing. Available Online: Https://Www.Eucast.Org/Ast_of_bacteria/ (Accessed on 20 January 2024). .
53. Schito, A.M.; Piatti, G.; Caviglia, D.; Zuccari, G.; Alfei, S. Broad-Spectrum Bactericidal Activity of a Synthetic Random Copolymer Based on 2-Methoxy-6-(4-Vinylbenzyloxy)-Benzylammonium Hydrochloride. *Int. J. Mol. Sci.* **2021**, *22*, 5021, doi:10.3390/ijms22095021.
54. Schito, A.M.; Schito, G.C.; Alfei, S. Synthesis and Antibacterial Activity of Cationic Amino Acid-Conjugated Dendrimers Loaded with a Mixture of Two Triterpenoid Acids. *Polymers (Basel).* **2021**, *13*, 521, doi:10.3390/polym13040521.

 doi:10.20944/preprints202603.0534.v1

55. Schito, A.M.; Alfei, S. Antibacterial Activity of Non-Cytotoxic, Amino Acid-Modified Polycationic Dendrimers against Pseudomonas Aeruginosa and Other Non-Fermenting Gram-Negative Bacteria. *Polymers (Basel).* **2020**, *12*, 1818, doi:10.3390/polym12081818.
56. Crémet, L.; Corvec, S.; Batard, E.; Auger, M.; Lopez, I.; Pagniez, F.; Dauvergne, S.; Caroff, N. Comparison of Three Methods to Study Biofilm Formation by Clinical Strains of Escherichia Coli. *Diagn. Microbiol. Infect. Dis.* **2013**, *75*, 252–255, doi:10.1016/j.diagmicrobio.2012.11.019.
57. Chandrasekhar, B.; Gor, R.; Ramalingam, S.; Thiagarajan, A.; Sohn, H.; Madhavan, T. Repurposing FDA-Approved Compounds to Target JAK2 for Colon Cancer Treatment. *Discover Oncology* **2024**, *15*, 226, doi:10.1007/s12672-024-01050-9.
58. Cui, M.; Li, Z.; Tang, R.; Jia, H.; Liu, B. Novel (E)-5-Styryl-2,2′-Bithiophene Derivatives as Ligands for β-Amyloid Plaques. *Eur. J. Med. Chem.* **2011**, *46*, 2908–2916, doi:10.1016/j.ejmech.2011.04.015.
59. Ammer, J.; Nolte, C.; Karaghiosoff, K.; Thallmair, S.; Mayer, P.; Devivie-Riedle, R.; Mayr, H. Ion-Pairing of Phosphonium Salts in Solution: C-H···halogen and C-H···π Hydrogen Bonds. *Chemistry - A European Journal* **2013**, *19*, doi:10.1002/chem.201204561.
60. Ceccacci, F.; Sennato, S.; Rossi, E.; Proroga, R.; Sarti, S.; Diociaiuti, M.; Casciardi, S.; Mussi, V.; Ciogli, A.; Bordi, F.; et al. Aggregation Behaviour of Triphenylphosphonium Bolaamphiphiles. *J. Colloid Interface Sci.* **2018**, *531*, 451–462, doi:10.1016/j.jcis.2018.07.067.
61. Alfei, S.; Marengo, B.; Valenti, G.; Domenicotti, C. Synthesis of Polystyrene-Based Cationic Nanomaterials with Pro-Oxidant Cytotoxic Activity on Etoposide-Resistant Neuroblastoma Cells. *Nanomaterials* **2021**, *11*, 977, doi:10.3390/nano11040977.
62. Alfei, S.; Piatti, G.; Caviglia, D.; Schito, A. Synthesis, Characterization, and Bactericidal Activity of a 4-Ammoniumbuthylstyrene-Based Random Copolymer. *Polymers (Basel).* **2021**, *13*, 1140, doi:10.3390/polym13071140.
63. Godoy, C.A.; Balic, I.; Moreno, A.A.; Diaz, O.; Arenas Colarte, C.; Bruna Larenas, T.; Gamboa, A.; Caro Fuentes, N. Antimicrobial and Antibiofilm Activity of Chitosan Nanoparticles Against Staphylococcus Aureus Strains Isolated from Bovine Mastitis Milk. *Pharmaceutics* **2025**, *17*, 186, doi:10.3390/pharmaceutics17020186.
64. Xu, W.; Lin, Z.; Cortez-Jugo, C.; Qiao, G.G.; Caruso, F. Antimicrobial Phenolic Materials: From Assembly to Function. *Angewandte Chemie International Edition* **2025**, *64*, doi:10.1002/anie.202423654.
65. Chen, X.; Lan, W.; Xie, J. Natural Phenolic Compounds: Antimicrobial Properties, Antimicrobial Mechanisms, and Potential Utilization in the Preservation of Aquatic Products. *Food Chem.* **2024**, *440*, 138198, doi:10.1016/j.foodchem.2023.138198.
66. Terekhova, N. V.; Tatarinov, D.A.; Shaihutdinova, Z.M.; Pashirova, T.N.; Lyubina, A.P.; Voloshina, A.D.; Sapunova, A.S.; Zakharova, L.Ya.; Mironov, V.F. Design and Synthesis of Amphiphilic 2-Hydroxybenzylphosphonium Salts with Antimicrobial and Antitumor Dual Action. *Bioorg. Med. Chem. Lett.* **2020**, *30*, 127234, doi:10.1016/j.bmcl.2020.127234.
67. Li, Y.-T.; Huang, L.; Wen, Z.-M.; Zhu, M.-T.; Zheng, X.-T.; Zhang, Z.-H.; Wang, Z.; Ni, C.-L. Synthesis, Crystal Structure, Optical and Antimicrobial Properties of 2-Nitrobenzyl Triphenylphosphonium Tetrabromocobaltate(II). *Journal of Structural Chemistry* **2024**, *65*, 243–255, doi:10.1134/S0022476624020033.
68. Andreeva, O. V.; Voloshina, A.D.; Lyubina, A.P.; Garifullin, B.F.; Strobykina, I.Yu.; Belenok, M.G.; Babaeva, O.B.; Babaev, V.M.; Aznagulov, R.F.; Saifina, L.F.; et al. Antimicrobial Activity of Triphenylphosphonium (TPP) Conjugates of Alkynyl–substituted Nucleic Bases and Their Analogues. *J. Antibiot. (Tokyo).* **2025**, *78*, 731–756, doi:10.1038/s41429-025-00864-1.
69. Andreeva, O. V.; Voloshina, A.D.; Lyubina, A.P.; Garifullin, B.F.; Sapunova, A.S.; Amerhanova, S.K.; Strobykina, I.Yu.; Belenok, M.G.; Babaeva, O.B.; Babaev, V.M.; et al. Triphenylphosphonium (TPP) Conjugates of 1,2,3-Triazolyl Nucleoside Analogues. Synthesis, Cytotoxicity and Antimicrobial Activity. *Medicinal Chemistry Research* **2025**, *34*, 367–391, doi:10.1007/s00044-024-03339-4.
70. Galkina, I. V.; Andriyashin, V. V.; Romanov, S.R.; Egorova, S.N.; Vorob'eva, N. V.; Shulaeva, M.P.; Pozdeev, O.K.; Litvinov, I.A.; Bakhtiyarova, Y. V. Synthesis, Structure and Antimicrobial Activity of Sterically Hindered Bis-Phosphonium Derivatives of 2,6-Di-Tert-Butyl-4-Methylphenol. *Mendeleev Communications* **2023**, *33*, 635–637, doi:10.1016/j.mencom.2023.09.014.

 doi:10.20944/preprints202603.0534.v1

71. Miller, W.R.; Arias, C.A. ESKAPE Pathogens: Antimicrobial Resistance, Epidemiology, Clinical Impact and Therapeutics. *Nat. Rev. Microbiol.* **2024**, *22*, 598–616, doi:10.1038/s41579-024-01054-w.
72. Kang, S.; Sunwoo, K.; Jung, Y.; Hur, J.K.; Park, K.-H.; Kim, J.S.; Kim, D. Membrane-Targeting Triphenylphosphonium Functionalized Ciprofloxacin for Methicillin-Resistant Staphylococcus Aureus (MRSA). *Antibiotics* **2020**, *9*, 758, doi:10.3390/antibiotics9110758.
73. Knauf, G.A.; Cunningham, A.L.; Kazi, M.I.; Riddington, I.M.; Crofts, A.A.; Cattoir, V.; Trent, M.S.; Davies, B.W. Exploring the Antimicrobial Action of Quaternary Amines against *Acinetobacter Baumannii*. *mBio* **2018**, *9*, doi:10.1128/mBio.02394-17.
74. Leggett, M.J.; Setlow, P.; Sattar, S.A.; Maillard, J.-Y. Assessing the Activity of Microbicides against Bacterial Spores: Knowledge and Pitfalls. *J. Appl. Microbiol.* **2016**, *120*, 1174–1180, doi:10.1111/jam.13061.
75. Maillard, J.-Y. Impact of Benzalkonium Chloride, Benzethonium Chloride and Chloroxylenol on Bacterial Antimicrobial Resistance. *J. Appl. Microbiol.* **2022**, *133*, 3322–3346, doi:10.1111/jam.15739.
76. Noel, D.J.; Keevil, C.W.; Wilks, S.A. Synergism versus Additivity: Defining the Interactions between Common Disinfectants. *mBio* **2021**, *12*, doi:10.1128/mBio.02281-21.
77. Worthing, K.A.; Marcus, A.; Abraham, S.; Trott, D.J.; Norris, J.M. Qac Genes and Biocide Tolerance in Clinical Veterinary Methicillin-Resistant and Methicillin-Susceptible Staphylococcus Aureus and Staphylococcus Pseudintermedius. *Vet. Microbiol.* **2018**, *216*, 153–158, doi:10.1016/j.vetmic.2018.02.004.
78. Buzón-Durán, L.; Alonso-Calleja, C.; Riesco-Peláez, F.; Capita, R. Effect of Sub-Inhibitory Concentrations of Biocides on the Architecture and Viability of MRSA Biofilms. *Food Microbiol.* **2017**, *65*, 294–301, doi:10.1016/j.fm.2017.01.003.
79. Rahmi, K.A.; Purwono, P.B.; Rochmanti, M. Benzalkonium Chloride Effectiveness as a Disinfectant against Hospital-Associated Methicillin-Resistant Staphylococcus Aureus (HA-MRSA). *Malays. J. Microbiol.* **2019**, doi:10.21161/mjm.180035.
80. Rahmi, K.A.; Purwono, P.B.; Rochmanti, M. Benzalkonium Chloride Effectiveness as a Disinfectant against Hospital-Associated Methicillin-Resistant Staphylococcus Aureus (HA-MRSA). *Malays. J. Microbiol.* **2019**, doi:10.21161/mjm.180035.
81. Akimitsu, N.; Hamamoto, H.; Inoue, R.; Shoji, M.; Akamine, A.; Takemori, K.; Hamasaki, N.; Sekimizu, K. Increase in Resistance of Methicillin-Resistant ***Staphylococcus Aureus*** **to β-Lactams Caused by Mutations Conferring Resistance to Benzalkonium Chloride, a Disinfectant Widely Used in Hospitals** . *Antimicrob. Agents Chemother.* **1999**, *43*, 3042–3043, doi:10.1128/AAC.43.12.3042.
82. Ferk, F.; Misik, M.; Hoelzl, C.; Uhl, M.; Fuerhacker, M.; Grillitsch, B.; Parzefall, W.; Nersesyan, A.; Micieta, K.; Grummt, T.; et al. Benzalkonium Chloride (BAC) and Dimethyldioctadecyl-Ammonium Bromide (DDAB), Two Common Quaternary Ammonium Compounds, Cause Genotoxic Effects in Mammalian and Plant Cells at Environmentally Relevant Concentrations. *Mutagenesis* **2007**, *22*, 363–370, doi:10.1093/mutage/gem027.
83. Matt, C.; Ilic Balestri, L.J.; Skillinghaug, B.; Odell, L.R. Synthesis of Phosphonium Ylides. *Comprehensive Organic Synthesis* **2025**, 601–648, doi:10.1016/B978-0-323-96025-0.00005-3.
84. Emery - Pharma The Time-Kill Kinetic Essay Available online: https://emerypharma.com/solutions/cell-microbiology-services/time-kill-kinetics-assay/ (accessed on 6 February 2026).
85. Time Kill Assay: Principles, Methods, and Antimicrobial Applications Available online: https://biologyinsights.com/time-kill-assay-principles-methods-and-antimicrobial-applications/ (accessed on 6 February 2026).
86. Schito, A.M.; Caviglia, D.; Piatti, G.; Zorzoli, A.; Marimpietri, D.; Zuccari, G.; Schito, G.C.; Alfei, S. Efficacy of Ursolic Acid-Enriched Water-Soluble and Not Cytotoxic Nanoparticles against Enterococci. *Pharmaceutics* **2021**, *13*, 1976, doi:10.3390/pharmaceutics13111976.
87. Alfei, S.; Caviglia, D.; Zorzoli, A.; Marimpietri, D.; Spallarossa, A.; Lusardi, M.; Zuccari, G.; Schito, A.M. Potent and Broad-Spectrum Bactericidal Activity of a Nanotechnologically Manipulated Novel Pyrazole. *Biomedicines* **2022**, *10*, 907, doi:10.3390/biomedicines10040907.
88. Schito, A.M.; Piatti, G.; Caviglia, D.; Zuccari, G.; Zorzoli, A.; Marimpietri, D.; Alfei, S. Bactericidal Activity of Non-Cytotoxic Cationic Nanoparticles against Clinically and Environmentally Relevant Pseudomonas Spp. Isolates. *Pharmaceutics* **2021**, *13*, 1411, doi:10.3390/pharmaceutics13091411.

 doi:10.20944/preprints202603.0534.v1

89. Alfei, S.; Caviglia, D.; Piatti, G.; Zuccari, G.; Schito, A.M. Bactericidal Activity of a Self-Biodegradable Lysine-Containing Dendrimer against Clinical Isolates of Acinetobacter Genus. *Int. J. Mol. Sci.* **2021**, *22*, 7274, doi:10.3390/ijms22147274.
90. Assessment of the Antimicrobial Activity Using a Time Kill Procedure (ASTM E2315-23Standard).
91. Baishya, H. Application of Mathematical Models in Drug Release Kinetics of Carbidopa and Levodopa ER Tablets. *J. Dev. Drugs* **2017**, *06*, doi:10.4172/2329-6631.1000171.
92. Alfei, S.; Grasso, F.; Orlandi, V.; Russo, E.; Boggia, R.; Zuccari, G. Cationic Polystyrene-Based Hydrogels as Efficient Adsorbents to Remove Methyl Orange and Fluorescein Dye Pollutants from Industrial Wastewater. *Int. J. Mol. Sci.* **2023**, *24*, 2948, doi:10.3390/ijms24032948.
93. Alfei, S.; Orlandi, V.; Grasso, F.; Boggia, R.; Zuccari, G. Cationic Polystyrene-Based Hydrogels: Low-Cost and Regenerable Adsorbents to Electrostatically Remove Nitrites from Water. *Toxics* **2023**, *11*, 312, doi:10.3390/toxics11040312.
94. Blondeau, J.; DeCory, H. In Vitro Time-Kill of Common Ocular Pathogens with Besifloxacin Alone and in Combination with Benzalkonium Chloride. *Pharmaceuticals* **2021**, *14*, 517, doi:10.3390/ph14060517.
95. Nordholt, N.; Kanaris, O.; Schmidt, S.B.I.; Schreiber, F. Persistence against Benzalkonium Chloride Promotes Rapid Evolution of Tolerance during Periodic Disinfection. *Nat. Commun.* **2021**, *12*, 6792, doi:10.1038/s41467-021-27019-8.
96. Kumari, S.; Jayakumar, S.; Bihani, S.C.; Shetake, N.; Naidu, R.; Kutala, V.K.; Sarma, H.D.; Gupta, G.D.; Sandur, S.K.; Kumar, V. Pharmacological Characterization of a Structurally New Class of Antibacterial Compound, Triphenyl-Phosphonium Conjugated Diarylheptanoid: Antibacterial Activity and Molecular Mechanism. *J. Biosci.* **2020**, *45*, 147, doi:10.1007/s12038-020-00113-7.
97. Saseendran Nair, S.; Anand, V.; De Silva, K.; Wiles, S.; Swift, S. The Antibacterial Potency and Antibacterial Mechanism of a Commercially Available Surface-Anchoring Quaternary Ammonium Salt (SAQAS)-Based Biocide in Vitro. *J. Appl. Microbiol.* **2022**, *133*, 2583–2598, doi:10.1111/jam.15729.
98. Xiao, Y.-H.; Chen, J.-H.; Fang, M.; Xing, X.-D.; Wang, H.; Wang, Y.-J.; Li, F. Antibacterial Effects of Three Experimental Quaternary Ammonium Salt (QAS) Monomers on Bacteria Associated with Oral Infections. *J. Oral Sci.* **2008**, *50*, 323–327, doi:10.2334/josnusd.50.323.
99. Alfei, S.; Caviglia, D. Prevention and Eradication of Biofilm by Dendrimers: A Possibility Still Little Explored. *Pharmaceutics* **2022**, *14*, 2016, doi:10.3390/pharmaceutics14102016.
100. Malone, M.; Bjarnsholt, T.; McBain, A.J.; James, G.A.; Stoodley, P.; Leaper, D.; Tachi, M.; Schultz, G.; Swanson, T.; Wolcott, R.D. The Prevalence of Biofilms in Chronic Wounds: A Systematic Review and Meta-Analysis of Published Data. *J. Wound Care* **2017**, *26*, 20–25, doi:10.12968/jowc.2017.26.1.20.
101. Fernández-Calderón, M.C.; Fernández-Babiano, I.; Navarro-Pérez, M.L.; Pazos-Pacheco, C.; Calvo-Cano, A. Biofilm Formation and Role of Other Pathogenic Factors in the Virulence of Staphylococcus Epidermidis Clinical Isolates. *Front. Cell. Infect. Microbiol.* **2025**, *15*, doi:10.3389/fcimb.2025.1630341.
102. Cheung, G.Y.C.; Otto, M. *Staphylococcus Epidermidis* —Key to Understanding Biofilms, Commensalism, and More. *J. Bacteriol.* **2025**, *207*, doi:10.1128/jb.00165-25.
103. Jonblat, S.; As-sadi, F.; Zibara, K.; Sabban, M. El; Dermesrobian, V.; Khoury, A. El; Kallassy, M.; Chokr, A. Staphylococcus Epidermidis Biofilm Assembly and Self-Dispersion: Bacteria and Matrix Dynamics. *International Microbiology* **2023**, *27*, 831–844, doi:10.1007/s10123-023-00433-2.
104. Sabaté Brescó, M.; Harris, L.G.; Thompson, K.; Stanic, B.; Morgenstern, M.; O'Mahony, L.; Richards, R.G.; Moriarty, T.F. Pathogenic Mechanisms and Host Interactions in Staphylococcus Epidermidis Device-Related Infection. *Front. Microbiol.* **2017**, *8*, doi:10.3389/fmicb.2017.01401.
105. Heilmann, C. Molecular Basis of Biofilm Formation by *Staphylococcus Epidermidis*. In *Medical Implications of Biofilms*; Cambridge University Press, 2003; pp. 110–135.
106. Percival, S.L.; Suleman, L.; Vuotto, C.; Donelli, G. Healthcare-Associated Infections, Medical Devices and Biofilms: Risk, Tolerance and Control. *J. Med. Microbiol.* **2015**, *64*, 323–334, doi:10.1099/jmm.0.000032.
107. Donlan, R.M.; Costerton, J.W. Biofilms: Survival Mechanisms of Clinically Relevant Microorganisms. *Clin. Microbiol. Rev.* **2002**, *15*, 167–193, doi:10.1128/CMR.15.2.167-193.2002.

 doi:10.20944/preprints202603.0534.v1

108. Foster, T.J.; Geoghegan, J.A.; Ganesh, V.K.; Höök, M. Adhesion, Invasion and Evasion: The Many Functions of the Surface Proteins of Staphylococcus Aureus. *Nat. Rev. Microbiol.* **2014**, *12*, 49–62, doi:10.1038/nrmicro3161.
109. STEPANOVIĆ, S.; VUKOVIĆ, D.; HOLA, V.; BONAVENTURA, G. DI; DJUKIĆ, S.; ĆIRKOVIĆ, I.; RUZICKA, F. Quantification of Biofilm in Microtiter Plates: Overview of Testing Conditions and Practical Recommendations for Assessment of Biofilm Production by Staphylococci. *APMIS* **2007**, *115*, 891–899, doi:10.1111/j.1600-0463.2007.apm_630.x.
110. O'Toole, G.A. Microtiter Dish Biofilm Formation Assay. *Journal of Visualized Experiments* **2011**, doi:10.3791/2437.
111. Zhou, C.; Wang, Y. Structure–Activity Relationship of Cationic Surfactants as Antimicrobial Agents. *Curr. Opin. Colloid Interface Sci.* **2020**, *45*, 28–43, doi:10.1016/j.cocis.2019.11.009.
112. Erick Ngehdzeka, C.; Menkem Elisabeth, Z. Bacterial Biofilm Eradication in Human Infections. In *Recent Advances in Bacterial Biofilm Studies - Formation, Regulation, and Eradication in Human Infections*; IntechOpen, 2024.
113. Wang, Y.; Bian, Z.; Wang, Y. Biofilm Formation and Inhibition Mediated by Bacterial Quorum Sensing. *Appl. Microbiol. Biotechnol.* **2022**, *106*, 6365–6381, doi:10.1007/s00253-022-12150-3.
114. Zhou, L.; Zhang, Y.; Ge, Y.; Zhu, X.; Pan, J. Regulatory Mechanisms and Promising Applications of Quorum Sensing-Inhibiting Agents in Control of Bacterial Biofilm Formation. *Front. Microbiol.* **2020**, *11*, doi:10.3389/fmicb.2020.589640.
115. Provencher, E.A.P.; Ehrig, M.R.; Cecere, A.G.; Cousins, S.C.; Maybin, M.A.; Meredith, T.C.; Miyashiro, T.I. Inhibition of Biofilm Formation by a Lipopolysaccharide-Associated Glycosyltransferase in the Bacterial Symbiont Vibrio Fischeri. *Frontiers in Bacteriology* **2023**, *2*, doi:10.3389/fbrio.2023.1254305.
116. Nguyen, A.N.X.; Thirapanmethee, K.; Audshasai, T.; Khuntayaporn, P.; Chomnawang, M.T. Insights into Molecular Mechanisms of Phytochemicals in Quorum Sensing Modulation for Bacterial Biofilm Control. *Arch. Microbiol.* **2024**, *206*, 459, doi:10.1007/s00203-024-04171-5.
117. Juszczuk-Kubiak, E. Molecular Aspects of the Functioning of Pathogenic Bacteria Biofilm Based on Quorum Sensing (QS) Signal-Response System and Innovative Non-Antibiotic Strategies for Their Elimination. *Int. J. Mol. Sci.* **2024**, *25*, 2655, doi:10.3390/ijms25052655.
118. Ma, R.; Hu, X.; Zhang, X.; Wang, W.; Sun, J.; Su, Z.; Zhu, C. Strategies to Prevent, Curb and Eliminate Biofilm Formation Based on the Characteristics of Various Periods in One Biofilm Life Cycle. *Front. Cell. Infect. Microbiol.* **2022**, *12*, doi:10.3389/fcimb.2022.1003033.
119. Fu, J.; Zhang, Y.; Lin, S.; Zhang, W.; Shu, G.; Lin, J.; Li, H.; Xu, F.; Tang, H.; Peng, G.; et al. Strategies for Interfering With Bacterial Early Stage Biofilms. *Front. Microbiol.* **2021**, *12*, doi:10.3389/fmicb.2021.675843.
120. Jefferson, K.K.; Goldmann, D.A.; Pier, G.B. Use of Confocal Microscopy To Analyze the Rate of Vancomycin Penetration through *Staphylococcus Aureus* Biofilms. *Antimicrob. Agents Chemother.* **2005**, *49*, 2467–2473, doi:10.1128/AAC.49.6.2467-2473.2005.
121. Tian, L.; Shi, S.; Zhang, X.; Han, F.; Dong, H. Newest Perspectives of Glycopeptide Antibiotics: Biosynthetic Cascades, Novel Derivatives, and New Appealing Antimicrobial Applications. *World J. Microbiol. Biotechnol.* **2023**, *39*, 67, doi:10.1007/s11274-022-03512-0.
122. Hu, T.; Wang, L. Vancomycin Resistance in Gram-Positive Infections: Evolutionary Strategies of Survival. *Arch. Microbiol.* **2026**, *208*, 148, doi:10.1007/s00203-025-04698-1.
123. Grooters, K.E.; Ku, J.C.; Richter, D.M.; Krinock, M.J.; Minor, A.; Li, P.; Kim, A.; Sawyer, R.; Li, Y. Strategies for Combating Antibiotic Resistance in Bacterial Biofilms. *Front. Cell. Infect. Microbiol.* **2024**, *14*, doi:10.3389/fcimb.2024.1352273.
124. Rivani, E.; Arfijanto, M.V.; Widodo, A.D.W. Vancomycin for Methicillin-Resistant Staphylococcus Aureus Biofilm Eradication Is Associated with the Emergence of Heterogeneous Vancomycin Intermediate Staphylococcus Aureus. *Int. J. Health Sci. (Qassim).* **2022**, 811–818, doi:10.53730/ijhs.v6nS9.12536.
125. Sharma, S.; Mohler, J.; Mahajan, S.D.; Schwartz, S.A.; Bruggemann, L.; Aalinkeel, R. Microbial Biofilm: A Review on Formation, Infection, Antibiotic Resistance, Control Measures, and Innovative Treatment. *Microorganisms* **2023**, *11*, 1614, doi:10.3390/microorganisms11061614.

 doi:10.20944/preprints202603.0534.v1

126. Singh, R.; Sahore, S.; Kaur, P.; Rani, A.; Ray, P. Penetration Barrier Contributes to Bacterial Biofilm-Associated Resistance against Only Select Antibiotics, and Exhibits Genus-, Strain- and Antibiotic-Specific Differences. *Pathog. Dis.* **2016**, *74*, ftw056, doi:10.1093/femspd/ftw056.
127. Pedroni, M.A.; Ribeiro, V.S.T.; Cieslinski, J.; Lopes, A.P. de A.; Kraft, L.; Suss, P.H.; Tuon, F.F. Different Concentrations of Vancomycin with Gentamicin Loaded PMMA to Inhibit Biofilm Formation of Staphylococcus Aureus and Their Implications. *Journal of Orthopaedic Science* **2024**, *29*, 334–340, doi:10.1016/j.jos.2022.11.022.
128. Shiri, M.; Ashrafi, F. The Bactericidal and Antibiofilm Effects of New Liposomes Containing Vancomycin Formulation Against Clinical Biofilm Positive Staphylococcus Aureus Isolates. *Appl. Biochem. Microbiol.* **2023**, *59*, 824–832, doi:10.1134/S0003683823060157.
129. Huang, Z.; Li, Y.; Yin, W.; Raby, R.B.N.; Liang, H.; Yu, B. A Magnetic-Guided Nano-Antibacterial Platform for Alternating Magnetic Field Controlled Vancomycin Release in Staphylococcus Aureus Biofilm Eradication. *Drug Deliv. Transl. Res.* **2025**, *15*, 1249–1264, doi:10.1007/s13346-024-01667-x.
130. Alharbi, O.; Alhazmi, K.; Gazzaz, M.; Almuhayya, S.; Aldehalan, F.; Sharif, A.; Redwan, B.; Alzain, M.; Alhazmi, W.; Altarawneh, H.; et al. A Review Vancomycin Role in Gram Positive Biofilm-Associated Infections: Challenges and Emerging Solutions. *Ther. Clin. Risk Manag.* **2025**, *Volume 21*, 1569–1578, doi:10.2147/TCRM.S541780.
131. Alharbi, O.; Alhazmi, K.; Gazzaz, M.; Almuhayya, S.; Aldehalan, F.; Sharif, A.; Redwan, B.; Alzain, M.; Alhazmi, W.; Altarawneh, H.; et al. A Review Vancomycin Role in Gram Positive Biofilm-Associated Infections: Challenges and Emerging Solutions. *Ther. Clin. Risk Manag.* **2025**, *Volume 21*, 1569–1578, doi:10.2147/TCRM.S541780.
132. Singh, R.; Sahore, S.; Kaur, P.; Rani, A.; Ray, P. Penetration Barrier Contributes to Bacterial Biofilm-Associated Resistance against Only Select Antibiotics, and Exhibits Genus-, Strain- and Antibiotic-Specific Differences. *Pathog. Dis.* **2016**, *74*, ftw056, doi:10.1093/femspd/ftw056.
133. Mu, W.B.; Yao, L.Q.; Guo, Z.Y.; Ma, Y.C.; Wang, F.; Yang, J.H. Enhancing Biofilm Disruption and Bactericidal Efficiency Using Vancomycin-Loaded Microbubbles in Sonodynamic Therapy. *JAC. Antimicrob. Resist.* **2025**, *7*, doi:10.1093/jacamr/dlaf045.
134. Borges, N.H.; Suss, P.H.; Ortis, G.B.; Dantas, L.R.; Tuon, F.F. Synergistic Activity of Vancomycin and Gentamicin Against Staphylococcus Aureus Biofilms on Polyurethane Surface. *Microorganisms* **2025**, *13*, 1119, doi:10.3390/microorganisms13051119.